Université d'Ottawa • University of Ottawa

Université d'Ottawa · University of Ottawa

FACULTÉ DES ÉTUDES SUPÉRIEURES ET POSTDOCTORALES

FACULTY OF GRADUATE AND POSTDOCTORAL STUDIES

AMIRI-HORMOZAKI, Kambiz
AUTEUR DE LA THÈSE - AUTHOR OF THESIS

M.A.Sc. (Civil Engineering)
GRADE - DEGREE

Department of Civil Engineering
FACULTÉ, ÉCOLE, DÉPARTEMENT - FACULTY, SCHOOL, DEPARTMENT

TITRE DE LA THÈSE - TITLE OF THE THESIS

Effects of Scaling of Earthquake Excitations on Dynamic Response of Reinforced Concrete Frame Buildings

Nove Naumoski / Murat Saatcioglu
DIRECTEUR DE LA THÈSE - THESIS SUPERVISOR

EXAMINATEURS DE LA THÈSE - THESIS EXAMINERS

M. Mohareb

H. Tanaka

J. Humar

J.-M. De Koninck, Ph.D.
LE DOYEN DE LA FACULTÉ DES ÉTUDES SUPÉRIEURES ET POSTDOCTORALES

SIGNATURE

DEAN OF THE FACULTY OF GRADUATE AND POSTDOCTORAL STUDIES

Effects of Scaling of Earthquake Excitations on Dynamic Response of Reinforced Concrete Frame Buildings

By

Kambiz Amiri-Hormozaki

A thesis
Presented to the University of Ottawa on partial fulfillment of the requirements for
Master of Applied Science in Civil Engineering

Department of Civil Engineering
University of Ottawa
Ottawa, Canada
K1N 6N5

November 2003

Your file Votre référence
ISBN: 0-494-01399-0
Our file Notre référence
ISBN: 0-494-01399-0

Dedicated to the Seven Martyrs of Hormozak;

Especially, My Grandfather and Grand Grandfather

تقدیم به شهدای سبعهٔ مزرعهٔ هرمزک

علی الخصوص پدر بزرگم و پدرش

Acknowledgments

I wish to express my sincere gratitude to my supervisors, Dr. Nove Naumoski for his help in devising the primary research plan and for his invaluable guidance during the course of this study, and Dr. Murat Saatcioglu for his kind support and excellent advice whenever the need arose. These two gentlemen made a remarkable difference in my life, which was not merely learning how to address research issues; for me, they set an example of modesty and ethical conduct in research.

I was very fortunate because most of the graduate courses I took during my program of studies were considerably related to my research topic. I would like to thank Dr's Hiroshi Tanaka, Murat Saatcioglu, Jag Humar, Magdi Mohareb, Erman Evgin, Gail Atkinson and Heng Khoo for sharing their knowledge by offering these courses.

My great and sincere acknowledgement is extended to the Bahá'í community of Canada for their love, continuous support and understanding during my studies in Canada.

Abstract

The objective of this study was to evaluate the effects of various scaling techniques of real accelerograms on the response of medium height moment-resisting reinforced concrete frame buildings. Detailed inelastic time-history analyses were conducted on three reinforced concrete frame buildings. Two of these buildings were six-storey buildings located in Vancouver, one of which was a ductile moment-resisting frame, and the other one was a nominally ductile frame. The third building was a five-storey nominally ductile moment-resisting frame building located in Montreal.

Two ensembles of real accelerograms recorded during strong earthquakes around the world were selected, one for Vancouver and the other for Montreal. Each ensemble contained 15 accelerograms. The frequency contents of the ensembles are representative for these two cities according to the 1995 edition of the seismic zoning maps of the National Building Code of Canada. Three scaling methods were used, i.e. (i) based on the spectral ordinate at the fundamental period of the building, (ii) based on the area under the spectral curve between the first and the second natural periods of vibration of the building (referred to as partial area), and (iii) based on the total area under the spectral curve throughout the whole period range (referred to as full area). Each scaling was conducted relative to the corresponding design spectrum (for Vancouver or Montreal) as prescribed in the 2005 edition of the National Building Code of Canada (NBCC 2005). In addition to the real accelerograms, three ensembles of artificial accelerograms for Vancouver, and three ensembles for Montreal were used for the purpose of comparison. One of these ensembles contained 15 accelerograms that were generated to be compatible with the corresponding (for Vancouver or Montreal) design spectrum. Each of the other two ensembles of artificial accelerograms consisted of 4 stochastically simulated accelerograms. Two levels of excitations were used in the analyses, i.e. the design level according to NBCC 2005, and twice the design level.

The response parameters that were investigated in this evaluation study were the interstorey drifts, curvature ductility demands in the beams, and curvature ductility demands in the columns of the buildings. For each ensemble of excitation motions and each level of excitation, statistical analyses were conducted to find the mean and the

mean plus one standard deviation levels of the response parameters. The evaluation of the scaling methods of the real accelerograms was based on these two statistical levels.

Based on the results from this study, the scaling of real records based on the area under the spectral curves within the predominant structural periods range is recommended for use in the design.

Table of Contents

List of Tables

List of Figures

Notation

E_c	Concrete modulus
E_s	Reinforcing steel modulus
f'_c	Cylinder compressive strength of concrete
f'_{cc}	Compression strength of confined concrete
f_s	Stress in reinforcing steel
f_{sm}	Specified maximum strength of reinforcing steel
f_y	Yield stress of reinforcing steel
f_{yh}	Yield strength of transverse reinforcing steel
f_u	Ultimate stress of reinforcing steel
F	Foundation factor (NBCC 1995)
F_a	Acceleration-based site coefficient (NBCC 2005)
F_v	Velocity-based site coefficient (NBCC 2005)
h_n	The height above the base of structure (NBCC 2005)
I	Seismic importance factor of structure (NBCC 1995)
I_E	Earthquake importance factor of structure (NBCC 2005)
M	Moment magnitude of earthquake
M_v	Factor to account for higher mode effect on base shear (NBCC 2005)
N	Total number of storeys (NBCC 1995)
PGA	Peak ground acceleration
PGV	Peak ground velocity
R	Focal distance of earthquake from the site of interest
R	Force modification factor representing inelastic capacity (NBCC 1995)

R_d	Ductility related force modification factor (NBCC 2005)
R_o	Overstrength related force modification factor (NBCC 2005)
S	Seismic response factor (NBCC 1995)
$S(T_a)$	The design spectral response acceleration (NBCC 2005)
$S_a(T)$	The 5% damped spectral response acceleration (NBCC 2005)
T	fundamental period of vibration of the building (NBCC 1995)
T_1	Fundamental (first) period of vibration of the building
T_2	Second period of vibration of the building
T_a	fundamental period of vibration of the building (NBCC 2005)
U	Factor representing level of protection based on experience (NBCC 1995)
v	Zonal velocity ratio (NBCC 1995)
V	Minimum lateral seismic force at the base of the structure (base shear)
W	Total weight of building for calculation of lateral seismic forces
ε_c	Compression strain of concrete
ε_{cc}	Strain at peak stress for confined concrete
ε_{cu}	Ultimate compression strain of concrete
$\varepsilon_{s,hrd}$	Hardening strain of reinforcing steel
ε_{sm}	Reinforcing steel strain at the maximum tensile stress
Φ_c	Material resistance factor for concrete
Φ_s	Material resistance factor for reinforcing steel
ρ	Confinement steel ratio

CHAPTER 1

INTRODUCTION

1.1 General

The seismic provisions of the latest edition of the National Building Code of Canada (NBCC 2005) specify seismic spectra for use in the design of buildings. These spectra are used to define the seismic forces for both the equivalent static method and the spectral analysis method. In the equivalent static method, the seismic forces correspond to those of the fundamental vibration mode of the building although a factor M_v is incorporated to account for higher mode effects. Two dynamic analysis methods are recognized by this code: In the spectral analysis method, the seismic forces associated with the predominant vibration modes (i.e., the first several modes) of the building are used in the design. The use of both these methods in the design of building structures is straightforward. In addition to this dynamic method, the NBCC 2005 seismic provisions allow time-history dynamic analysis for more important and irregular buildings as the preferred method. For the purpose of dynamic time-history analysis, acceleration time-histories of the ground motion are needed. The code explicitly requires that the design acceleration time-histories of the ground motions (referred to as design accelerograms) should be compatible with the design spectrum. However, the term "compatibility" is not defined by the code and it is left to the designer to decide. Also, the code does not specify what type of design accelerograms should be used, whether artificially generated to satisfy the design spectrum, or real accelerograms which can be scaled to some parameters in order to be close to the design spectrum. Currently, there are several methods and computer programs for generation of artificial accelerograms compatible with design (i.e., target) spectra, which are widely used in design of buildings. However, there are concerns in terms of the use of artificial accelerograms. Several research studies have indicated significant potential problems associated with the use of artificial accelerograms in the design of structures, which can lead to inaccurate estimates of the expected performance of the structures when subjected to design earthquake ground motions. In addition, with the use of artificial accelerograms, one of the most important feature of earthquake motions, the randomness of the motions, is lost. In contrast to the use of artificial accelerograms, some building codes explicitly require the use of recorded accelerograms during strong earthquakes (referred to as real accelerograms) and prescribe a specific method for the scaling of these accelerograms for use in the design of building structures, New Zealand code (NZS 4203:1992) is an example.

1.2 Objective and Scope of the Study

The objective of this study is to evaluate the effects of various techniques of scaling real accelerograms on the response of moment-resisting reinforced concrete buildings. Detailed time-history analyses were conducted on the following three reinforced concrete frame buildings:

(i) Six-storey ductile moment-resisting frame building located in Vancouver,

(ii) Six-storey nominally ductile moment-resisting frame building located in Vancouver, and

(iii) Five-storey nominally ductile moment-resisting frame building located in Montreal.

Two ensembles of real accelerograms recorded during strong earthquakes around the world were selected, one for Vancouver and the other for Montreal. Each ensemble contained 15 accelerograms. The frequency contents of the ensembles are representative for these two cities according to the 1995 edition of the seismic zoning maps of the National Building Code of Canada.

Three scaling methods were used:

(i) based on the spectral ordinate at the fundamental period of the building,

(ii) based on the area under the spectral curve between the first and the second natural vibration periods of the building (referred to as partial area), and

(iii) based on the total area under the spectral curve throughout the whole period range (referred to as full area).

Each scaling was conducted relative to the corresponding design spectrum (for Vancouver or Montreal) as given in NBCC 2005.

In addition to the real accelerograms, three ensembles of artificial accelerograms for Vancouver, and three ensembles for Montreal were used for the purpose of comparison. One of these ensembles contained 15 accelerograms that were generated to be compatible with the corresponding (for Vancouver or Montreal) design spectrum. Each of the other two ensembles of artificial accelerograms consisted of 4 stochastically simulated accelerograms. Two levels of excitations were used in the analyses, i.e. the design level according to NBCC 2005, and twice the design level.

The response parameters that were investigated in this evaluation study were the interstorey drifts, curvature ductility demands in the beams, and curvature ductility demands in the columns of the buildings. For each ensemble of excitation motions, statistical analyses were conducted to find the mean and the mean plus one standard deviation levels of the response parameters. The evaluation of the scaling methods of the accelerograms was based on these two statistical levels.

1.3 Outline of the Thesis

Chapter 2 presents a review of the available literature related to objective of this study, i.e. the effects of the use of real and artificial accelerograms on the response of building structures, as well as the available scaling methods of accelerograms. The main characteristics of the three buildings that were analyzed in this study are described in Chapter 3. Chapter 4 describes the computer program used for the inelastic dynamic analysis and the modelling of the buildings. The stress-strain models for concrete and steel are also presented in Chapter 4. Chapter 5 describes the ensembles of the excitation time-histories used in the analyses of the buildings. Detailed discussion of the analyses and the results of this study are given in Chapter 6. Finally, Chapter 7 presents the main conclusions that resulted from the analyses of the buildings.

CHAPTER 2

LITERATURE REVIEW

2.1 Code Requirements for Use of Earthquake Excitations

The seismic provisions of the latest edition of the National Building Code of Canada (NBCC 2005) require the use of design spectrum compatible accelerograms in the time-history analysis of building structures. However, no criteria for the compatibility between the accelerogram and the design spectrum are prescribed. Also, these provisions do not specify what kind of accelerograms should be used, i.e. artificially generated accelerograms, or recorded accelerograms during strong earthquakes that are referred to as real accelerograms.

The seismic provisions of the California Office of Statewide Health Planning and Development (OSHPD 1991) also require the use of design spectrum compatible accelerograms for the time-history analysis of building structures. According to these provisions, the 5%-damped response spectrum of the artificial accelerogram should essentially envelope the design spectrum without falling below the design spectrum by more than 10% at any period (Naeim and Lew 1995).

The New Zealand Standard (NZS 4203:1992) is quite specific. This code requires the use of at least three scaled real earthquake records rather than artificially generated accelerograms compatible with the design spectrum. According to this code, "scaling shall be such that over the period range of interest for the structure being analyzed, the

5%-damped spectrum of the earthquake record does not differ significantly from the design spectrum".

The requirements of the European Standard for Bridges (Eurocode 8 1998) are also very specific. According to this code, "at least three pairs of horizontal ground motion time-history components should be used. The pairs should be selected from recorded events with magnitudes, source distances, and mechanisms consistent with those that define the design seismic action. When the required number of pairs of appropriate recorded ground motions is not available, appropriate simulated accelerograms may be used in replacement of the missing recorded motions".

2.2 Review of Past Research

The number of studies related to the evaluation of the effects of artificial accelerograms that are compatible with the design spectrum and scaled real records to satisfy prescribed compatibility criteria (between the spectrum of the real records and the design spectrum) is very limited. Most of these studies are conducted using single-degree-of-freedom systems (Martínez-Rueda 1998, Tremblay and Atkinson 2001). Design spectrum compatible time-histories are usually generated by modifying the amplitudes and the frequency content of real records to match the target design spectrum. Naeim and Lew (1995) reported that, despite the attractiveness of such time-histories to designers, they are inconsistent with the purpose and the definition of design spectrum. The rationale is that the design spectrum envelopes the effects of multiple earthquake events and not of a single event. Therefore, considering a single event which matches the design spectrum within the whole period range is not realistic. The authors used design compatible time-histories to investigate the response of a six-storey base-isolated hospital building located in south central Los Angeles. They reported an extreme caution in dealing with artificial time-histories in the seismic design of structures, because such time-histories may represent unrealistic velocity, displacement, and frequency content.

Atkinson and Beresnev (1998) simulated ground motion time-histories compatible with the Uniform Hazard Spectra (UHS) with probability of exceedance of 10% in 50 years, for different locations in Canada. The authors used seismological models for performing the time-history simulations.

Tremblay and Atkinson (2001) simulated 2% in 50 year UHS compatible time-histories, and used these time-histories in a study of a bilinear single-degree-of-freedom (SDOF) system. In that study, the authors assumed that the simulated motions are adequate, and discussed the dependency between the force modification factor, R, on one hand, and the ductility level, the damage law, the structural period, and the tectonic region, on the other hand.

Martínez-Rueda (1998) recommended the use of scaled real earthquake records rather than artificial design spectrum compatible time-histories. The author investigated the displacement ductility demand of a bilinear SDOF system subjected to ensembles of scaled real accelerograms. The study resulted in a system of spectrum intensity scales for scaling purposes of real records.

Shome et al. (1998) studied the displacement ductility demand and damage index of a five-storey, four-bay moment-resisting steel frame. The authors considered four different ensembles of real earthquake records. Each ensemble consisted of 20 accelerograms from relatively narrow magnitude and distance ranges. All the records were recorded on stiff soil in California. In spite of having very close magnitude and distance values within each ensemble, the authors observed a wide dispersion in the nonlinear response parameters of the five-storey building. . These dispersion measures were equal to, or greater than that of SDOF spectral acceleration responses. The authors observed, however, that when the records in each ensemble were scaled to the ensemble median spectral acceleration at the fundamental period of the structure, the same values of the median responses but with reduced variability were obtained. Given this, for the purpose of the investigation of the nonlinear effects of a given magnitude and distance event on a structure, the authors suggested to first use an attenuation law to establish the median spectral acceleration, and then to scale the records from approximately the same magnitude and distance to this spectral acceleration. The authors concluded that this procedure could reduce the number of records needed to obtain the median response by a factor of about 4.

CHAPTER 3

DESCRIPTION OF BUILDINGS

3.1 Building #1

This building was originally designed by Naumoski and Heidebrecht (1997) as part of a pilot project on the seismic level of protection of reinforced concrete frame structures, which is described in Heidebrecht (1997). Detailed description of the building, design approach, and reinforcement ratios are given in Naumoski and Heidebrecht (1997). This section presents the geometrical and design information for Building #1 that are of interest for this study.

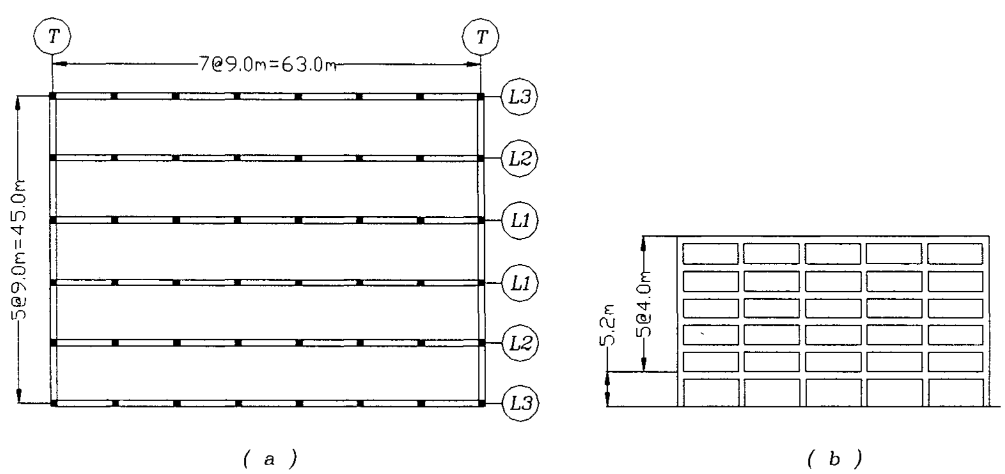

Fig. 3.1 Buildings #1 and #2; (a) Plan of floors, (b) Elevation of transverse frames

The building is a six storey moment-resisting reinforced concrete frame structure located in Vancouver BC. The plan of the floors and elevation of transverse frames are shown in Fig. 3.1. The storey heights are 4.0 m, except for the first storey which has a height of 5.2 m. The transverse frames have 5 spans, and the longitudinal frames have 7 spans. The spans are 9 m long in both the transverse and longitudinal directions.

For the transverse direction, the two end moment-resisting frames (marked T in the figure) provide all of the earthquake resistance, with the other columns in the building carrying only gravity loads. The design of the transverse frames is dominated by lateral loads, since each frame carries one half of the lateral load of the entire building while carrying only the gravity load of the adjacent half-bay. For the longitudinal direction, the earthquake resistance is shared among six moment-resisting frames (marked L1, L2, and L3 in the figure). With this configuration of structural systems, the design of the longitudinal frames is governed by both gravity and lateral loads. The floor system consists of a one-way slab spanning in the transverse direction, supported by the beams in the longitudinal frames; the slab is cast integrally with the beams.

In this study, only the transverse frames were used. This is primarily because, as mentioned above, the design of the transverse frames is dominated almost exclusively by lateral seismic loads The cross sections of all the columns of the transverse frames are 90 cm $\times$ 90 cm, and those of the beams are 50 cm $\times$ 110 cm. The reinforcement of the columns and beams of the transverse frames is shown in Table 3.2.The building is designed as an office building located in Vancouver. The building foundation is assumed to be on rock The design is conducted according to the 1995 edition of the National Building Code of Canada (NBCC 1995). The transverse frames are designed as ductile moment-resisting frames using force reduction factor R = 4. The design parameters used in the calculation of the base shear coefficient (i.e., the base shear expressed as a percentage of the weight of the building) are summarized in Table 3.1. As shown in this table, the base shear coefficient is 5.81%. This base shear is increased by approximately 14% due to torsional effects, which results in a total base shear of 6.62%. The strengths of the concrete and reinforcing steel used in the design are, respectively, $f_c' = 30$ MPa and $f_y = 400$ MPa, except that $f_y = 300$ MPa for the slabs. The concrete modulus is $E_c = 27\,000$ MPa, and the steel modulus is $E_s = 200\,000$ MPa. The CSA A23.3-94 material standard (CSA 1994) is used for reducing moments of inertia of beams and columns due to cracking, i.e. using 40% and 70% of the gross EI for beams and columns respectively. Since the seismic excitations used in this study correspond to the provisions of NBCC 2005 (draft version), base shear coefficient and design parameters according to the new code are also presented in Table 3.1. The new code specifies design spectra having a 2% in 50 year probability of exceedance for each city across the country. Again, the building is assumed to be located in Vancouver region. Firm ground conditions (i.e., "reference ground condition" designated as soil type C in NBCC 2005) is considered. For these conditions, the base shear for the building according to the new code is 6.60% of the total weight. Given this, the design base shear according to NBCC 2005 is approximately equal to that used in the design of the building according to NBCC 1995.

Table 3.1 Equivalent static force parameters and base shear coefficients for Building #1

NBCC 1995	$T=0.1N$	$S=1.5/T^{1/2}$	R	U	F	I	v	V/W	1.14×V/W
	0.6	1.9365	4	0.6	1	1	0.2	5.81%	6.62%
NBCC 2005	$T_a=0.075h_n^{3/4}$	$S(T_a)$	R_d	R_o	M_v	I_E	F_a	F_v	V/W
	0.84	0.4488	4	1.7	1	1	1	1	6.60%

Table 3.2 Percentages of longitudinal reinforcing steel for beams and columns of Building #1

Floor level	Columns		Beams	
	Exterior	Interior	Top	Bottom
Roof	0.99	1.68	0.36	0.36
5th	0.99	0.99	0.55	0.36
4th	0.99	1.48	0.82	0.55
3rd	0.99	2.07	1.15	0.82
2nd	1.33	2.42	1.27	1.02
1st	1.73	2.42	1.40	1.15
Base	2.96	3.46	N/A	N/A

Note: The percentages shown in this table are expressed in terms of gross cross-sectional dimensions

3.2 Building #2

This building is a design variation of building #1 designed by Naumoski and Heidebrecht (1997). The only difference is that this variation was designed as a moment-resisting frame with nominal ductility, i.e. R=2. The geometrical properties and member sizes are identical to those of Building #1. However, the reinforcement ratios for this building are significantly larger than those of Building #1. The building is also located in Vancouver and is on rock foundation. As shown in Table 3.3, the base shear for the transverse frames is 11.62% of the total weight of the building. In the design, this base shear was increased by approximately 14% due to torsional effects, which resulted in a total design base shear of 13.25%, which is twice as much as that for Building #1. The base shear according to NBCC 2005, for "moderately ductile" moment-resisting frame is 12.84% of the total weight. As for Building #1, only the transverse frames were used in the analysis since the design of the frames is governed almost exclusively by lateral seismic loads. The longitudinal reinforcement ratios for the columns and beams of the transverse frames are given in Table 3.4.

Table 3.3 Equivalent static force parameters and base shear coefficients for Building #2

NBCC 1995	T= 0.1N	S= $1.5/T^{1/2}$	R	U	F	I	v	V/W	1.14×V/W
	0.6	1.936	2	0.6	1	1	0.2	11.62%	13.25%
NBCC 2005	T_a= $0.075h_n^{3/4}$	$S(T_a)$	R_d	R_o	M_v	I_E	F_a	F_v	V/W
	0.84	0.4488	2.5	1.4	1	1	1	1	12.84%

Table 3.4 Percentages of longitudinal reinforcing steel for beams and columns of Building #2

Floor level	Columns		Beams	
	Exterior	Interior	Top	Bottom
Roof	1.04	1.04	0.55	0.27
5^{th}	1.38	1.73	1.02	0.76
4^{th}	1.38	2.47	1.53	1.27
3^{rd}	1.98	2.96	2.00	1.64
2^{nd}	1.98	3.46	2.36	2.18
1^{st}	2.47	3.46	2.55	2.36
Base	5.93	5.93	N/A	N/A

Note: The percentages shown in this table are expressed in terms of gross cross-sectional dimensions

3.3 Building #3

This building was originally designed by Dincer (2003). It is a five storey moment-resisting reinforced concrete frame. The building was designed for Ottawa following the NBCC 2005 provisions. All the storey heights are 4.0 m. The longitudinal frames have 5 spans, and the transverse frames have 3 spans. Each span is 6.0 m long in both the longitudinal and the transverse direction. The plan and the elevation of the transverse frames are shown in Fig. 3.2.

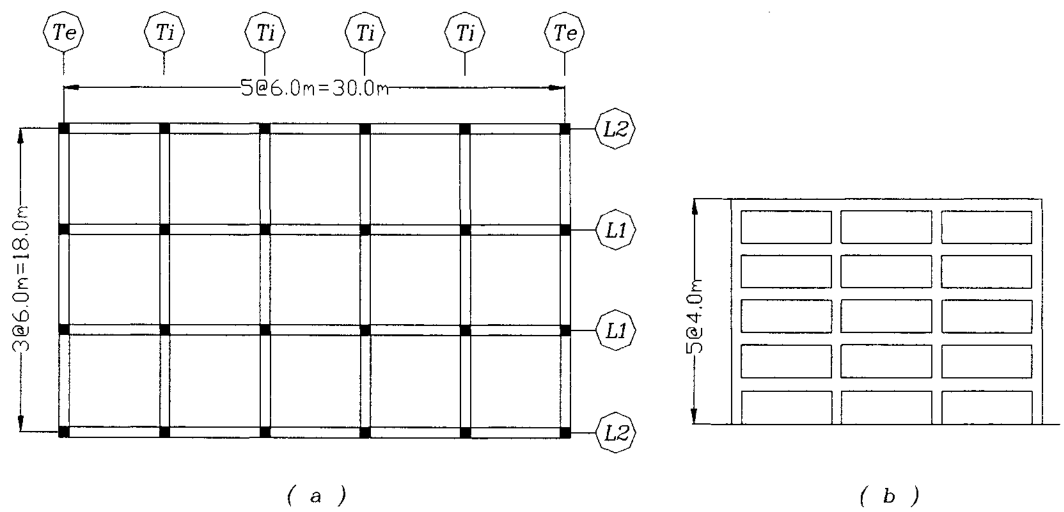

Fig. 3.2 Building #3; (a) Plan of floors, (b) Elevation of transverse frames

Only the transverse frames were designed for this building. In this study, only one interior transverse frame, marked 'T_i' in Fig. 3.2 is used. For this frame, the exterior and the interior columns are 40.0 cm×40.0 cm and 45.0 cm×45.0 cm respectively. The beams are 30.0 cm×45.0 cm except for the fifth floor beams which are 30.0 cm×40.0 cm.

The foundation of the building is on so-called reference soil, designated type C in NBCC 2005. The frames were designed as moderately ductile moment-resisting frames according to NBCC 2005. The design parameters and the base shear coefficients are given in Table 3.5. It can be seen that the design base shear is 6.86% of the total weight of the structure for Ottawa. However, the building is assumed to be located in Montreal which will lead to a base shear coefficient of 7.31% according to Table 3.5. The base shear coefficients for the two cities are close enough to allow the assumption that the building designed for Ottawa is also adequate for Montreal. The concrete and steel properties used in the design are the same as those for Building #1. The longitudinal reinforcement ratios for the columns and beams of frame T_i are shown in Table 3.6.

Table 3.5 Equivalent static force parameters and base shear coefficients for Building #3

NBCC 2005 (Ottawa)	$T_a = 0.075h_n^{3/4}$	$S(T_a)$	R_d	R_o	M_v	I_E	F_a	F_v	V/W
	0.71	0.2402	2.5	1.4	1	1	1	1	6.86%
NBCC 2005 (Montreal)	$T_a = 0.075h_n^{3/4}$	$S(T_a)$	R_d	R_o	M_v	I_E	F_a	F_v	V/W
	0.71	0.2560	2.5	1.4	1	1	1	1	7.31%

Table 3.6 Percentages of longitudinal reinforcing steel for beams and columns of Building #3

Floor level	Columns		Beams	
	Exterior	Interior	Top	Bottom
Roof	1.50	1.98	0.75	0.33
4th	1.50	1.98	1.11	0.44
3rd	1.50	1.98	1.11	0.44
2nd	1.50	1.98	1.11	0.44
1st	1.50	1.98	1.11	0.44
Base	1.50	1.98	N/A	N/A

Note: The percentages shown in this table are expressed in terms of gross cross-sectional dimensions

CHAPTER 4

BUILDING MODELS AND MODELLING PARAMETERS

4.1 Introduction

In this study, the program IDARC (Inelastic Damage Analysis of Reinforced Concrete) (Kunnath et al. 1994) was used for nonlinear dynamic analyses of the buildings. The program requires an analytical model of the structure, and a seismic excitation time-history. This chapter describes the models of the buildings and the modelling parameters (i.e., constitutive models for concrete and steel, and moment-curvature relationships).

4.2 Main Characteristics of the IDARC Model

The program IDARC (Kunnath et al. 1994) was developed for two-dimensional analysis of reinforced concrete structures. Therefore, the structural model is represented by a 2-D model. Among the different types of elements incorporated in IDARC, the beam-column element was used for the development of the analytical models of the selected buildings. This element is represented by a simple flexural spring in which shear deformation effects are included. Axial deformation effects, in addition to flexural and shear deformations are included in columns, but no interaction between bending moment and axial load is taken into account. The effects of axial deformations are ignored in beams. Given these assumptions, each beam has four degrees of freedom (rotation and vertical displacements at each end) and each column has six degrees of freedom. The flexural model takes into account a combination of concentrated plasticity at the member ends and distributed elasticity along the member. Concentrated end plasticity is defined by tri-linear moment curvature relationships (see later in this chapter). The modelling of shear deformations is accomplished by means of an equivalent spring that acts in series with the flexural spring. The stiffness of a given member is represented by the equivalent stiffness of the shear and flexural springs. The program takes into account P-Δ effects.

4.3 Building Models

As mentioned earlier, from each building only one frame was analyzed. This is primarily because IDARC has been developed for 2-D analysis. The beams and the columns were assumed as line elements, connected at their ends to form frames. The models of buildings are shown in Fig. 4.1.

Since the geometrical properties of Building #1 and Building #2 are the same, the geometry of the models of these two buildings are practically identical. However, because of the different reinforcement ratios for the frames in Building #1 and Building #2, there are significant differences between the models of the buildings in terms of the strength and deformation properties of the column and beam elements. These properties are represented by the moment-curvature relationships (discussed later in this chapter) that are specified for each section of the beam and column elements.

In each model, the masses are lumped at the nodal points, which are located at the connection points of beams and columns. Gravity loads are applied as distributed loads on beams. Gravity loads due to the self weights of the columns are applied as concentrated loads at nodes. Gravity loads caused by transverse beams are added to the concentrated loads. This is the case for all the nodes of Building #3 frame and exterior nodes of Buildings #1 and #2 frames.

4.4 Constitutive Models for Materials

As mentioned above, for the purpose of the nonlinear analysis of the buildings, tri-linear moment-curvature relationships are required for the end-sections of each element of the models. These relationships depend on the geometrical properties of the members and the constitutive models of the concrete and the reinforcing steel. Presented hereafter are the main characteristics of these constitutive models and the development of moment-curvature relationships.

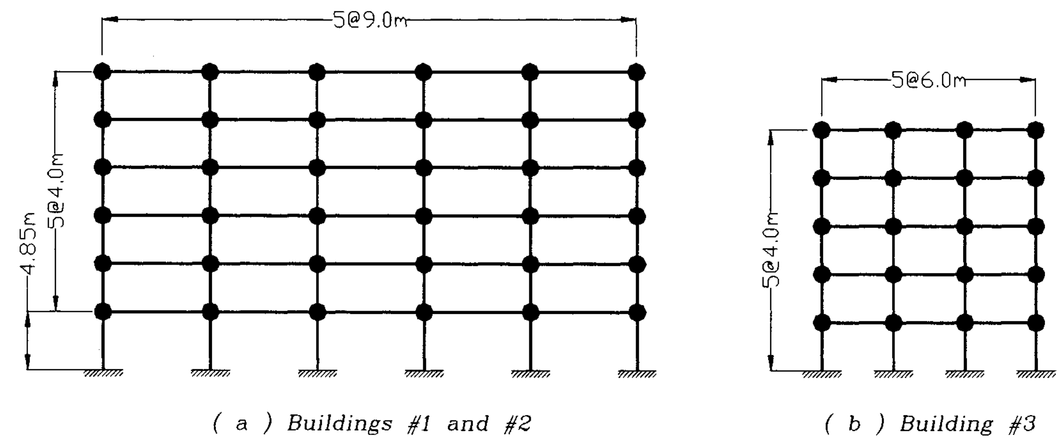

Fig. 4.1 Building models; (a) Buildings #1 and #2, (b) Building #3

4.4.1 Constitutive Model for Confined Concrete

In any analysis of reinforced concrete buildings, it is essential that the constitutive model of the concrete includes the effect of the confinement. There are a number of strain-stress models for confined concrete. The model used in this study was that proposed by Mander et al. (1988). This model was developed for concrete sections confined by transverse reinforcement and subjected to uniaxial compressive loading. The model is shown in Fig. 4.2. Detailed explanations for this model can be found in Mander et al. (1988), and Paulay and Priestley (1992); therefore, these will not be repeated here. However, it is useful to comment briefly on the main characteristics of this model and on the parameters used in this study. As shown in Fig. 4.2, the Mander model for confined concrete is represented by the curve that encloses the shaded area. This curve is defined by the confined concrete compressive strength, f'_{cc}, the confined concrete compressive stress, ε_{cc}, and the ultimate compressive strain, ε_{cu}, that corresponds to the first hoop fracture. As described in Mander (1988), and Paulay and Priestley (1992), these parameters can be determined using the compression strength of the concrete, f'_c, the compressive strain of the concrete, ε_c, the confinement ratio, ρ, the yield strength of the transverse (i.e., horizontal) reinforcement, f_{yh}, and the strain of the transverse reinforcement, ε_{sm}, at the maximum tensile stress. In this study, f'c was taken 30 MPa, as used in the design for all three buildings. The values for the confinement ratios, ρ, were calculated from the transverse reinforcement obtained in the design. The characteristics of both the longitudinal and transverse reinforcement are shown in the constitutive model of the reinforcing steel that follows.

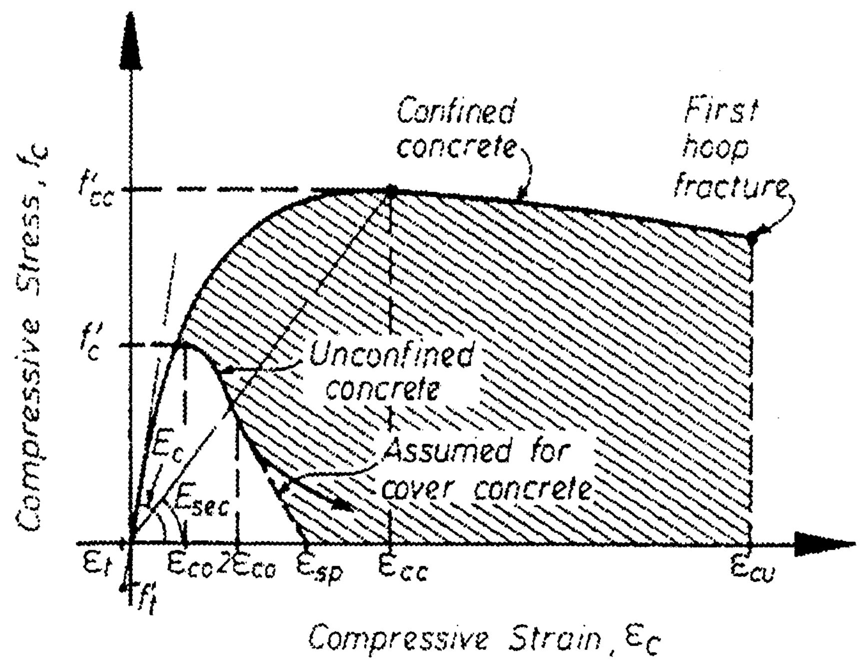

Fig. 4.2 Confined concrete strain-stress model (Priestly et al. 1996)

4.4.2 Constitutive Model for Reinforcing Steel

A typical stress-strain curve for reinforcing steel is shown in Fig. 4.3. The curve consists of four segments, i.e. an initial linear elastic segment with modulus of 200 GPa, followed by a yield plateau, strain-hardening region, and finally a range in which stress drops off until fracture happens. In this study, the yield strength f_y=400 MPa is used. The strain at which the hardening begins was taken as $\varepsilon_{s,hrd}$ = 0.01, and the strain at the maximum stress was taken as ε_u = 0.1. The ultimate stress was taken f_u = 1.5·f_y, as suggested by Priestley (1996) for typical North American reinforcement

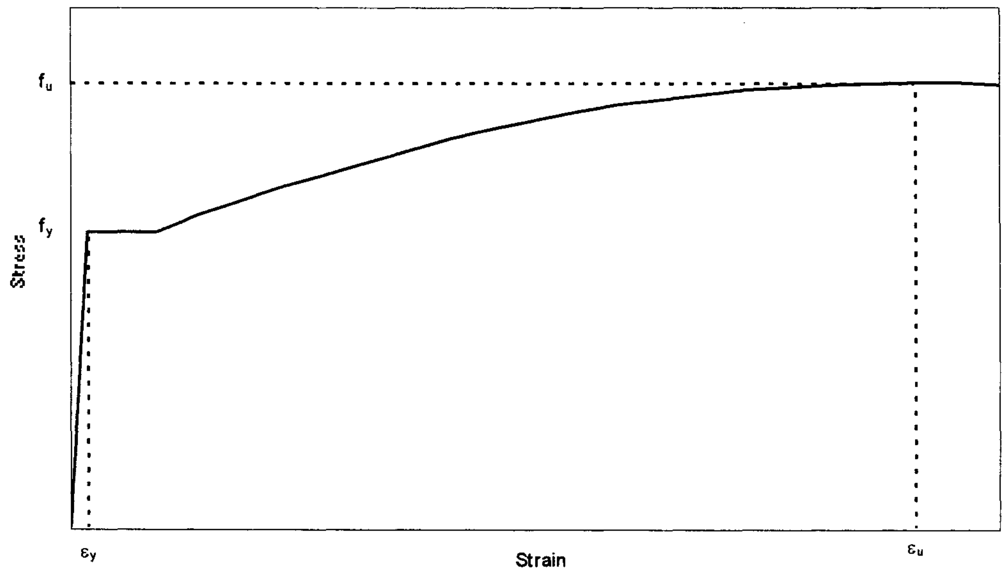

Fig. 4.3 Reinforcing steel stress-strain model

4.5 Moment-Curvature Relationships

Tri-linear moment curvature relationships for the frames of Buildings #1 and #2 were originally calculated by Naumoski and Heidebrecht (1998a) using the computer program FIBER developed by Naumoski (1996). For the frame of Building #3, the moment–curvature relationships were computed using the program RCSection 1.3 (Goudreault, 2000). For the purpose of verification, moment-curvature relationships were also computed for several members of Building #1 using the program RCSection 1.3. It was found that the results of both programs were quite close. The ultimate curvature, which is representative of the maximum deformation capacity of a section, corresponds to one of the following two cases, whichever is reached first: (i) the specified ultimate compression strain, ε_{cu}, in the extreme fiber of the section, or (ii) the specified maximum strength, f_u, of the longitudinal reinforcing bars. A typical moment-curvature relationship is shown in Fig. 4.4. The computed moment-curvature relationship was simplified into a tri-linear envelope for use in IDARC. The first segment corresponds to the uncracked stiffness, the second segment corresponds to the region between cracking and yielding, and the third segment corresponds to the post-yielding range.

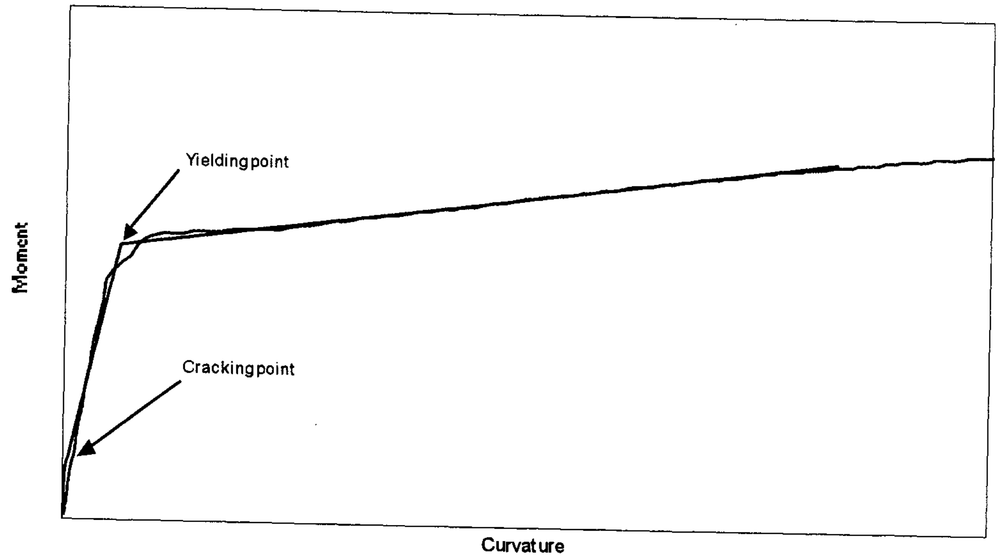

Fig. 4.4 Tri-linear moment curvature relationship

The calculation of the moment-curvature relationships for all of the column sections was based on the gravity loads on the columns. However, the axial load during earthquake motions varies with time. Naumoski and Heidebrecht (1998) investigated the effects of such variation on the response parameters, such as curvature ductilities and drifts, and found that these effects are not significant and could be neglected.

A sensitivity analysis conducted by Bayani-keyvani (2003), to investigate the effects of different stress-strain models on the moment-curvature relationships showed that the final results obtained from different models, especially the yield curvatures, were relatively close.

4.6 Hysteretic Modelling

During an earthquake event, different structural components may experience numerous deformation excursions beyond the yielding points. The inelastic response of the structural members depends significantly on the hysteretic model. IDARC uses tri-linear moment-curvature envelope with the ability to model the hysteretic characteristics such as stiffness degradation, strength deterioration, and pinching behaviour. The hysteretic behaviour under repeated loading is controlled by four user-defined parameters called hysteretic parameters. A brief description of these parameters is given hereafter.

4.6.1 Stiffness Degrading Parameter

This parameter defines the stiffness decay during seismic response. As shown in Fig. 4.5, all unloading paths on the primary curve target a common point. This point is defined by the initial stiffness of the section prescribed by the moment-curvature envelope of the member, and HC (the indicator of stiffness decay) as a multiplier of the yielding moment. Based on experimental tests, the typical range for HC is between 1.5 and 3.0 (Kunnath et al. 1994). The two extreme bounds of 0.10 and 10.0 are associated with severe degradation and negligible degradation respectively. In general, a larger value of HC means smaller stiffness degradation and vice versa. The nominal value for HC is 2.0 (Kunnath et al. 1994) and this value was used in this study.

4.6.2 Strength Deterioration Parameter

The modelling of strength deterioration is also illustrated in Fig. 4.5. The strength deterioration is controlled by two related parameters, ductility-based strength decay parameter, HBD, and energy-based strength decay parameter, HBE. The values of both the HBD and HBE parameters range between 0.0 for negligible deterioration and 0.40 for severe deterioration. In this study, the value of 0.10 was used for both parameters to simulate the nominal degradation effects (Kunnath et al. 1994).

4.6.3 Pinching Control Parameter

Pinching behaviour is either due to bond slip or crack closing (see Fig. 4.5). This effect is introduced in IDARC by the HS parameter, which ranges from 0.1 for extremely pinched loops to 1.0 for no pinching condition. The pinching effects are modelled by the program through the change of the unloading and reloading paths, when these paths are within the range between $HS \times M_y$ and $HS \times (-M_y)$, where M_y is the yielding moment of the section. The nominal value of HS=0.5 was used in this study as suggested by Kunnath et al. (1994).

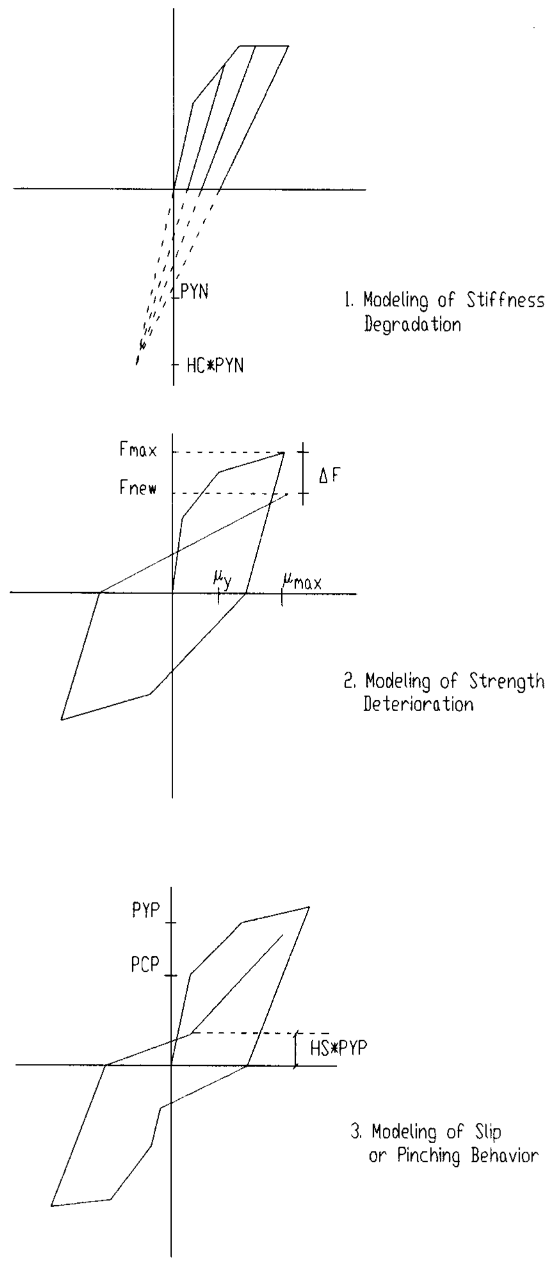

Fig. 4.5 Hysteretic model control parameters

CHAPTER 5

INPUT GROUND MOTIONS

5.1 Introduction

Since the objective of this study is to investigate the effects of scaling of excitation motions on the response of frame buildings, artificial accelerograms compatible with the design spectra, and actual earthquake accelerograms that were scaled using different scaling methods were used as excitation motions in the dynamic analysis of the selected buildings. Based on the method for the generation of the artificial accelerograms, two types of such accelerograms were used. One of these methods provides accelerograms compatible with the design spectrum (Naumoski 2001), and the other method is based on a stochastic simulation technique for the generation of artificial accelerograms (Atkinson and Beresnev 1998). In addition to the artificial accelerograms, actual earthquake accelerograms, that were scaled using different scaling techniques, were used in the dynamic analyses of the frames. This chapter describes both the artificial accelerograms and the techniques for scaling of the actual accelerograms.

5.2 Artificial Accelerograms Compatible with the Design Spectrum

NBCC 2005 (draft version) allows nonlinear dynamic analysis using ground motion time-histories compatible with the design acceleration spectrum. Also, there are other codes that require the use of such accelerograms. As an example, Naeim and Lew (1995) refer to the Uniform Building Code (International Conference of Building

Officials; ICBO 1991, 1994). In some codes, the concept of compatibility is defined as having a response spectrum which is not below the design spectrum more than a prescribed percentage. For example, Naeim and Lew (1995) quote the specifications of the California Office of Statewide Health Planning and Development (OSHPD 1991). The criterion of compatibility is not specified in the draft version of NBCC 2005. As required by the code, "the ground motion histories used in the Numerical Integration Linear Time History Method shall be compatible with a response spectrum constructed from the design spectral acceleration values".

In this study, the program SYNTH (Naumoski 2001) was used for the generation of artificial accelerograms compatible with the regional design spectra. To generate an artificial accelerogram, the program requires: (i) the target spectrum (representing the design spectrum), and (ii) an initial accelerogram. This program iteratively modifies the Fourier amplitudes of the initial accelerogram until its spectrum matches the target spectrum. In general, the initial accelerogram can be any accelerogram; it is needed just to start the generation process. However, it is preferred to use recorded accelerograms of real earthquakes as initial accelerograms (Naumoski 2001). It is useful to mention that the generated accelerogram maintains some of the characteristics of the initial accelerogram. Namely, the phase angles of the Fourier components of the generated accelerogram are the same as those of the initial accelerogram. Also, the generated accelerogram has a strong motion duration which is similar to that of the initial accelerogram. This is a very useful feature of the SYNTH program, because the strong motion duration of the generated accelerogram is controlled by the user. For example, if an artificial accelerogram with a long strong motion duration is required, then the user should select an initial accelerogram with a long strong motion duration, and vice versa. It is also useful to mention that the overall shape of the generated accelerogram is very similar to the shape of real accelerograms.

Since the investigated buildings are located in Vancouver and Montreal, two target spectra were used in this study, one for Vancouver and another for Montreal. Both these represent design spectra and were developed as specified in the seismic provisions of NBCC 2005. The code specifies the peak ground acceleration (PGA) and spectral acceleration values $S_a(T)$ for periods of 0.2 s, 0.5 s, 1.0 s and 2.0 s for the reference ground conditions, that is designated as site class C in the code. Both the PGA and $S_a(T)$ are for a probability of exceedance of 2% in 50 years. The code spectral values and the PGA values for Vancouver and Montreal are given in Table 5.1, and the "extended" design spectra are shown in Fig. 5.2. Since NBCC 2005 specifies spectral values only for periods of 0.2 s and above, some extensions of the spectra were done for periods below 0.2 s. This is needed because it is not possible to generate artificial accelerogram using SYNTH if the target spectrum is not defined throughout the whole period range. For Vancouver, spectral values for periods (T) between 0.1 s and 0.2 s were assumed to be the same. For periods below 0.1 s, the code spectrum was represented by a linear segment (in linear scale) that decreases from the spectral value at T=0.1 s to the PGA value at T=0.03 s, and a constant plateau at PGA for all periods below 0.03 s. For Montreal, the spectral values between T=0.03 s at T=0.2 s were taken to be the same as that of the code spectral value for T=0.2 s. For periods below 0.03 s, the spectrum linearly decreases from the spectral value at T=0.03 s to the PGA value at T=0.02 s, and a plateau at the PGA value for periods below 0.02 s. Detailed explanations on the background for these extensions are given in Naumoski (2002a, 2002b).

Two ensembles of artificial accelerograms were developed for this study, one of which was compatible with the design spectrum for Vancouver, and the other one compatible with the design spectrum for Montreal. The initial accelerograms used in the generation of the artificial accelerograms for Vancouver are given in Table 5.4, and those used for the generation of the artificial accelerograms for Montreal are given in Table 5.5. Each of the generated ensembles consists of 15 accelerograms. The ensemble for Vancouver will be referred to as ADCV ensemble (Artificial Design Compatible for Vancouver), and the ensemble for Montreal will be referred to as ADCM (Artificial Design Compatible for Montreal). For illustration, Fig. 5.1shows samples of the generated artificial accelerograms for Vancouver and Montreal. The matching of the spectra of the sample artificial accelerograms and the design spectra for Vancouver and Montreal is illustrated in Fig. 5.2. It can be seen from this figure that the spectra of the generated accelerograms and the design spectra are quite close.

Table 5.1 Spectral accelerations for 5% damping and PGA values for Vancouver and Montreal as specifed in NBCC 2005.

City	$S_a(0.2)$ (g)	$S_a(0.5)$ (g)	$S_a(1.0)$ (g)	$S_a(2.0)$ (g)	PGA (g)
Vancouver	1.0	0.68	0.34	0.18	0.50
Montreal	0.69	0.34	0.14	0.048	0.43

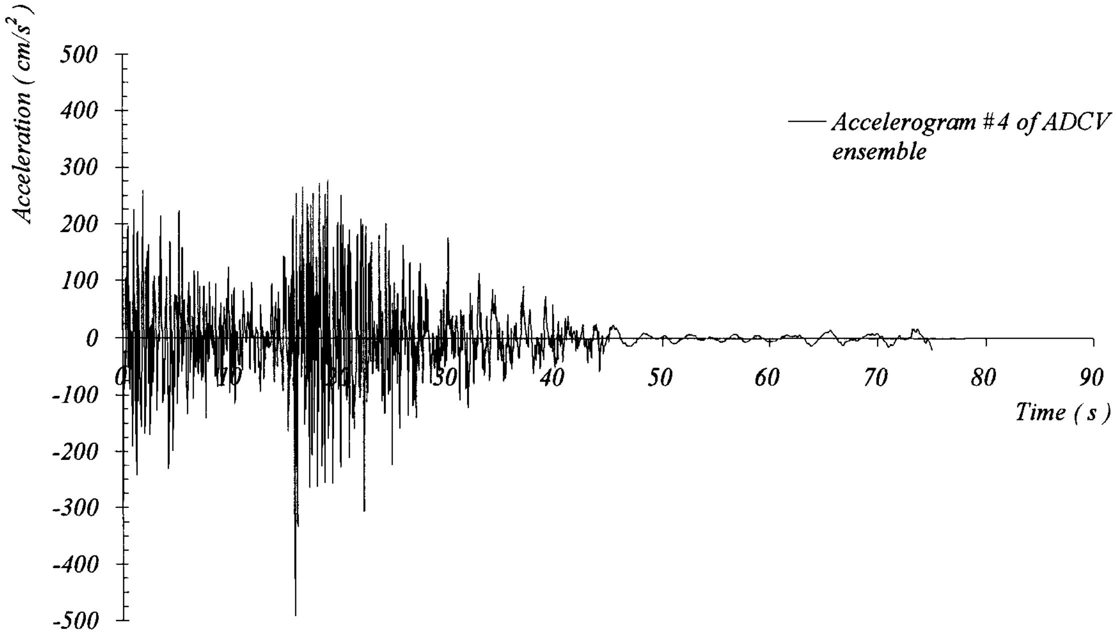

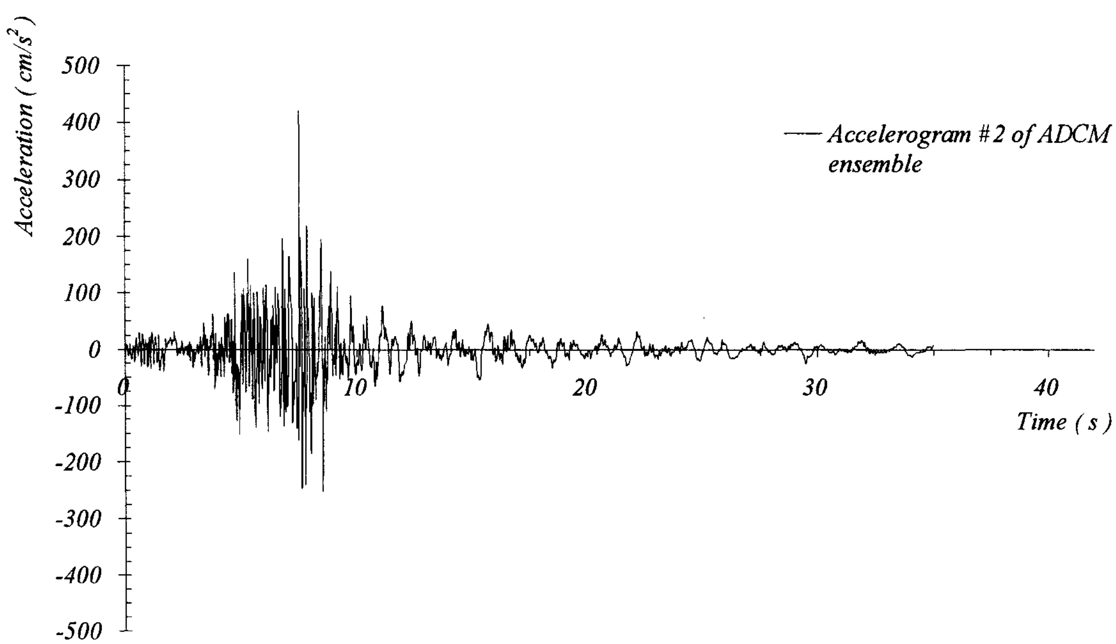

Fig. 5.1 Samples of the ensembles of artificial accelerograms for Vancouver and Montreal

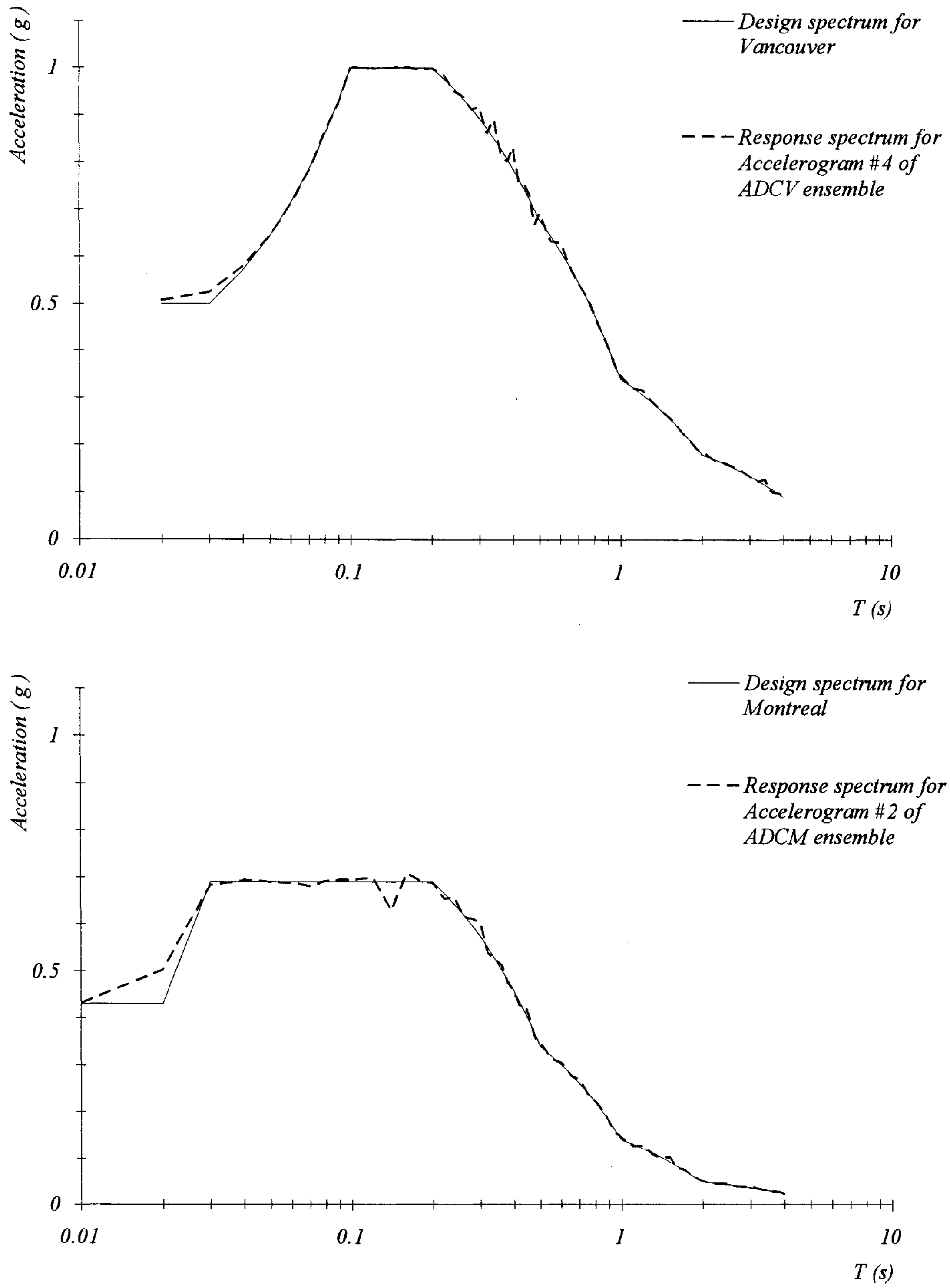

Fig. 5.2 Response spectra of samples of the generated artificial accelerograms for Vancouver and Montreal and corresponding design spectra

5.3 Simulated Earthquake Accelerograms Based on Seismological Models

Two ensembles for Vancouver and two other ensembles for Montreal were also examined during this research. Each ensemble consists of only four trials of moment-distance scenarios. These time-histories were simulated by Tremblay and Atkinson (2001) to be compatible with the median 2% in 50 year Uniform Hazard Spectra (UHS) provided by Geological Survey of Canada (GSC) (Adams et al. 1999). Ordinates of the target UHS are given in Table 5.2. A comparison of Table 5.1 and Table 5.2 shows that the target spectra for the artificial accelerograms of section 5.2 are practically the same as the spectra discussed above.

Table 5.2 2% / 50 year UHS ordinates in (g) (Tremblay and Atkinson 2001).

Period (s)	0.1	0.15	0.2	0.3	0.4	0.5	1.0	2.0
Vancouver	0.83	1.00	1.00	0.87	0.76	0.67	0.34	0.18
Montreal	0.68	0.71	0.69	0.50	0.39	0.34	0.14	0.048

Detailed explanation of simulation methodology is given by Tremblay and Atkinson (2001), and Atkinson and Beresnev (1998). However, a brief review of these two references is presented here. The first step in the simulation of 2% in 50 year UHS compatible accelerograms is the selection of scenario events. For western British Columbia, events of M6.5 and 7.2 represent short and long period ranges of the UHS respectively. For eastern Canada, events of M6.0 and M7.0 can exhibit short and long period hazards respectively. Based on the seismicity rates of the site area, different distances might be considered for the short and long period events. The simulation uses stochastic point-source method. First, a random time series of windowed white noise with zero mean amplitude and spectral amplitude of unity is generated. The duration of the window is specified by the appropriate magnitude-distance scenario. Then, the Fourier spectrum of this time series is multiplied (i.e., convoluted in time domain) by the source spectrum as a function of magnitude, attenuation with distance, and the site amplification function. The resulting spectrum is transferred back into time domain. (Tremblay and Atkinson 2001, Atkinson and Beresnev 1998)

Some parameters of the simulated time-histories for these two cities are shown in Table 5.3. It can be seen that there is a so-called "fine-tuning", factor which is specified by the authors in order to provide compatibility with the target spectra.

Table 5.3 Ensembles of "fine-tuned" simulated ground motions

Vancouver						Montreal					
Ensemble Name	M	R (km)	Factor	Trial No.	PGA (g)	Ensemble Name	M	R (km)	Factor	Trial No.	PGA (g)
M6.5R30	6.5	30	1.0	1	0.53	M6.0R30	6.0	30	0.85	1	0.36
				2	0.53					2	0.44
				3	0.58					3	0.40
				4	0.39					4	0.37
M7.2R70	7.2	70	1.0	1	0.25	M7.0R70	7.0	70	0.90	1	0.27
				2	0.26					2	0.26
				3	0.23					3	0.31
				4	0.25					4	0.26

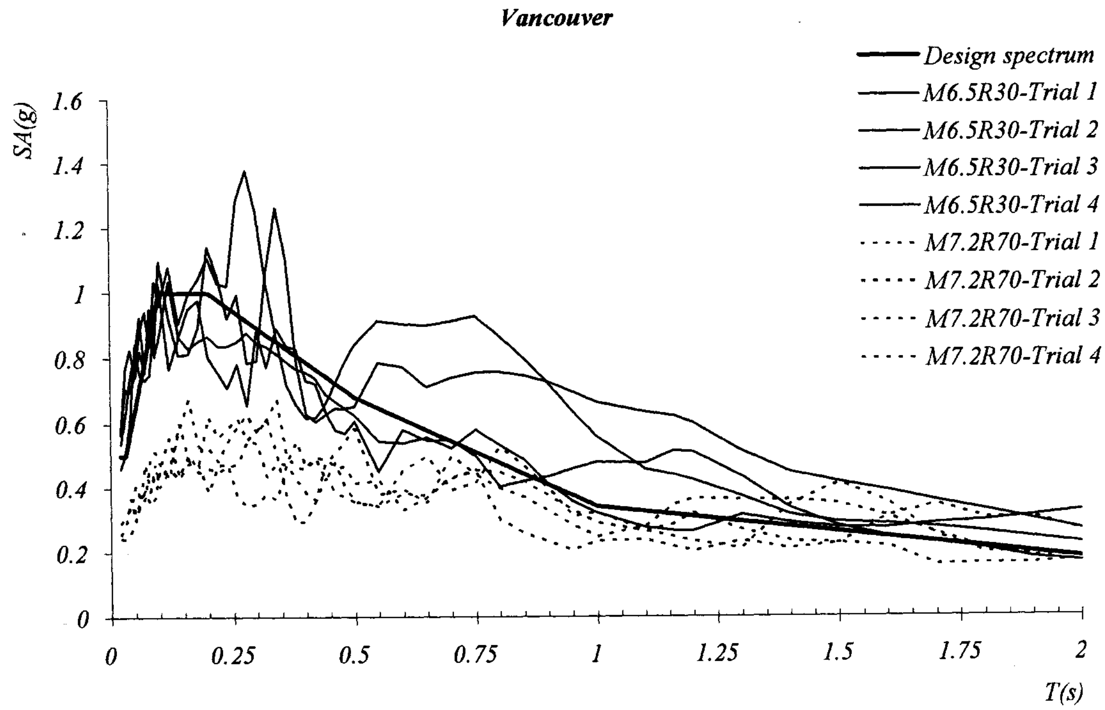

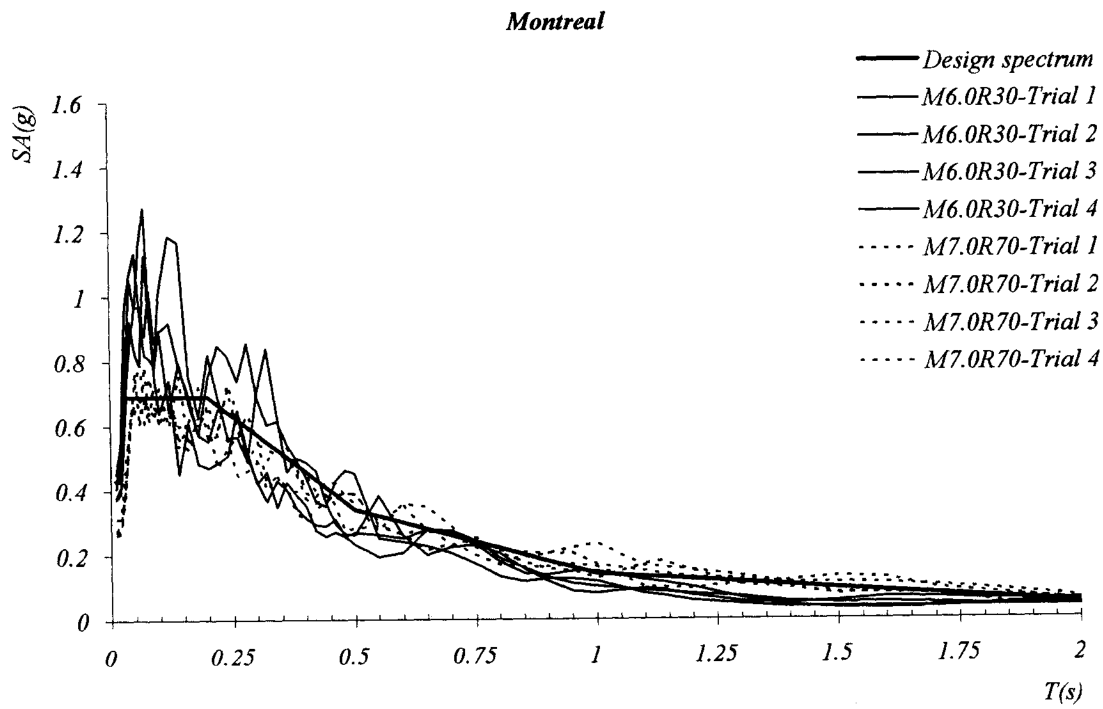

Fig. 5.3 Acceleration response spectra for all simulated time-histories, 5% damping

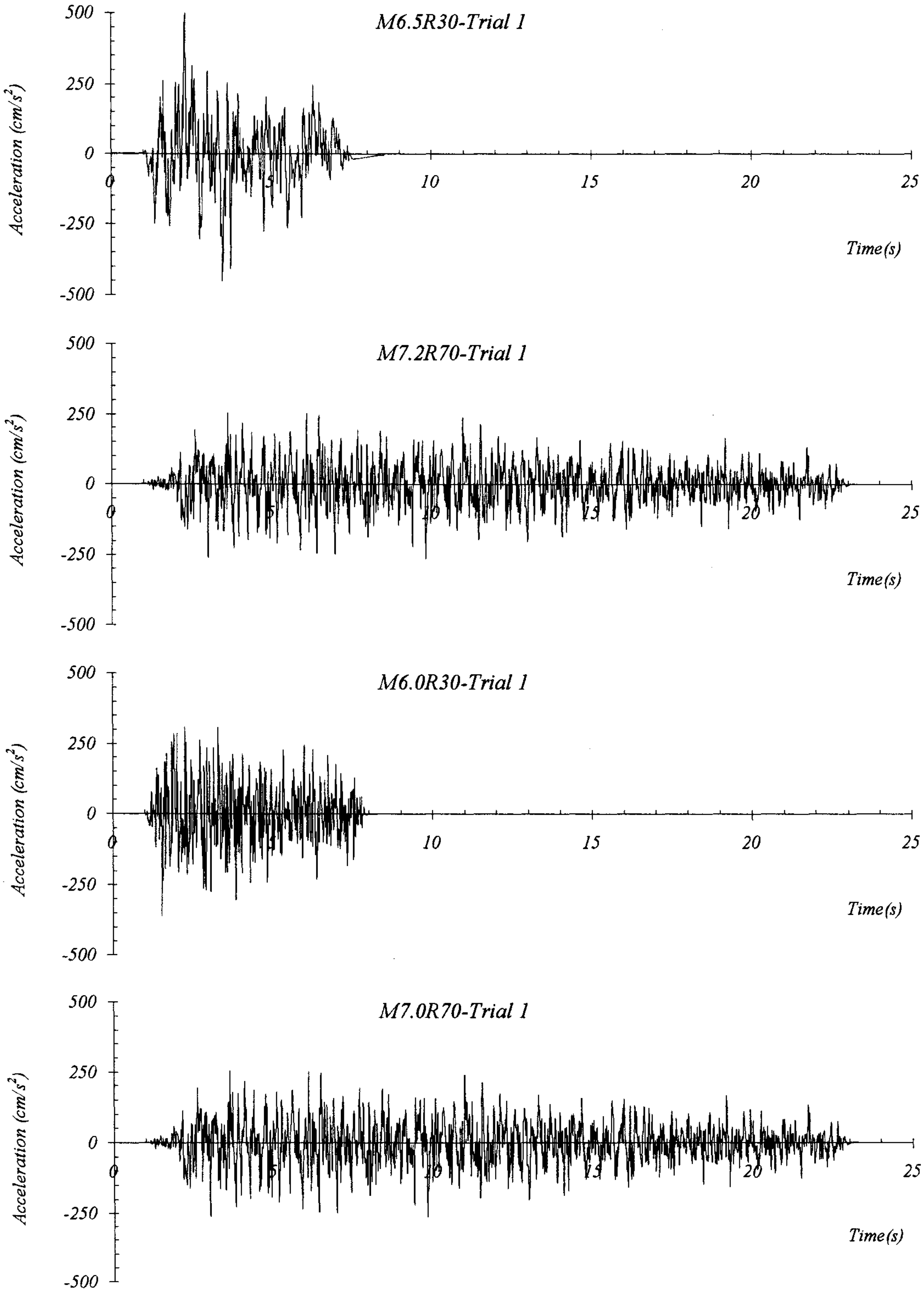

Fig. 5.4 Samples of the four different sets of the simulated time-histories

5.4 Real Accelerograms

When real accelerograms are used for dynamic analysis of a structure in a given region, it is important that these accelerograms are representative of the seismic motions for that region. One of the approaches is to use actual accelerograms recorded in other regions but having frequency content that is expected for the location of the structure. It is known that the peak ground acceleration to peak ground velocity ratio (PGA / PGV) of seismic motion is an indicator of the frequency content of the motion. PGA/PGV ratios around 1.0 are characteristic for seismic motions in western Canada, and PGA/PGV ratios about 2.0 and higher are characteristic of seismic motions in eastern Canada (NBCC 1995). Based on the PGA/PGV ratios, Naumoski et al. (1988) selected three ensembles of records. Two of these ensembles were used in this study. Each of these ensembles consists of 15 accelerograms. The accelerograms of one of the ensembles have PGA/PGV ratios between 0.8 and 1.2; this ensemble was used in the dynamic analysis of the Buildings #1 and #2 (located in Vancouver), and will be referred to as RW (Real records for West). The accelerograms of the other ensemble have PGA/PGV ratios between 1.7 and 2.6; this ensemble was used in the dynamic analysis of the Building #3 (located in Montreal), and will be referred to as RE (Real records for East). The accelerograms of the RW and the RE ensembles are listed in Table 5.4 and Table 5.5 respectively.

Table 5.4 Ensemble of Real records for West (RW) with intermediate PGA/PGV ratios (Naumoski et al. 1988)

No.	Earthquake description	Date	Site	Mag.	Epic. dist. (km)	Comp.	PGA (g)	PGV (m/s)	PGA/PGV	Soil Cond.
1	Imperial Valley California	May 18 1940	El Centro	6.6	8	S00E	0.348	0.334	1.04	Stiff soil
2	Kern County California	Jul. 21 1952	Taft Lincoln School Tunnel	7.6	56	S69E	0.179	0.177	1.01	Rock
3	Kern County California	Jul. 21 1952	Taft Lincoln School Tunnel	7.6	56	N21E	0.156	0.157	0.99	Rock
4	Boreggo Mtn. California	Apr. 8 1968	San Onofre SCE Power Plant	6.5	122	N57W	0.046	0.042	1.10	Stiff soil
5	San Fernando California	Apr. 8 1968	San Onofre SCE Power Plant	6.5	122	N33E	0.041	0.037	1.11	Stiff soil
6	San Fernando California	Feb. 9 1971	3838 Lankershim Blvd. L.A.	6.4	24	S90W	0.150	0.149	1.01	Rock
7	San Fernando California	Feb. 9 1971	Hollywood Storage P.E. Lot, L.A.	6.4	35	N90E	0.211	0.211	1.00	Stiff soil
8	San Fernando California	Feb. 9 1971	3407 6th Street L.A.	6.4	39	N90E	0.165	0.166	0.99	Stiff soil
9	San Fernando California	Feb. 9 1971	Griffith Park Observatory, L.A.	6.4	31	S00W	0.180	0.205	0.88	Rock
10	San Fernando California	Feb. 9 1971	234 Figueroa St., L.A.	6.4	41	N37E	0.199	0.167	1.19	Stiff soil
11	Near E. Coast of Honshu Japan	Nov. 16 1974	Kashima Harbor Works	6.1	38	N00E	0.070	0.072	0.97	Stiff soil
12	Near S. Coast of Honshu Japan	Aug. 2 1971	Kushiro Central Wharf	7.0	196	N90E	0.078	0.068	1.15	Stiff soil
13	Monte Negro Yugoslavia	Apr. 15 1979	Albatros Hotel, Ulcinj	7.0	17	N00E	0.171	0.194	0.88	Rock
14	Mexico Earthquake	Sep. 19 1985	El Suchil, Guerrero Array	8.1	230	S00E	0.105	0.116	0.91	Rock
15	Mexico Earthquake	Sep. 19 1985	La Villita, Guerrero Array	8.1	44	N90E	0.123	0.105	1.17	Rock

Table 5.5 Ensemble of Real records for East (RE) with high PGA/PGV ratios (Naumoski et al. 1988)

No.	Earthquake description	Date	Site	Mag.	Epic. dist. (km)	Comp.	PGA (g)	PGV (m/s)	PGA/PGV	Soil Cond.
1	Parkfield California	Jun 27 1966	El Centro	5.6	7	N65W	0.269	0.145	1.86	Rock
2	Parkfield California	Jun 27 1966	Taft Lincoln School Tunnel	5.6	5	N85E	0.343	0.255	1.70	Rock
3	San Francisco California	Mar 22 1957	Taft Lincoln School Tunnel	5.25	11	S80E	0.105	0.046	2.28	Rock
4	San Francisco California	Mar 22 1957	San Onofre SCE Power Plant	5.25	17	S09E	0.085	0.051	1.67	Stiff Soil
5	Helena Montana	Oct. 31 1935	San Onofre SCE Power Plant	6.0	8	N00E	0.146	0.072	2.03	Rock
6	Lystle Creek	Sep. 12 1970	3838 Lankershim Blvd. L.A.	5.4	15	S25W	0.198	0.096	2.06	Rock
7	Oroville California	Aug. 1 1975	Hollywood Storage P.E. Lot, L.A.	5.7	13	N53W	0.084	0.044	1.91	Rock
8	San Fernando California	Feb. 9 1971	3407 6th Street L.A.	6.4	4	S74W	1.075	0.577	1.86	Rock
9	San Fernando California	Feb. 9 1971	Griffith Park Observatory, L.A.	6.4	26	S21W	0.146	0.085	1.72	Rock
10	Nahanni N.W.T Canada	Dec. 23 1985	234 Figueroa St., L.A.	6.9	7.5	LONG	1.101	0.462	2.38	Rock
11	Central Honshu Japan	Feb. 26 1971	Kashima Harbor Works	5.5	27	TRANS	0.151	0.059	2.56	Stiff Soil
12	Near E. Coast of Honshu, Japan	Aug. 2 1971	Kushiro Central Wharf	5.8	33	N00E	0.146	0.060	2.43	Stiff Soil
13	Honshu, Japan	May 11 1972	Albatros Hotel, Ulcinj	5.4	4	N00E	0.270	0.111	2.43	Stiff Soil
14	Monte Negro Yugoslavia	Apr. 9 1979	El Suchil, Guerrero Array	5.4	12.5	N00E	0.042	0.016	2.63	Rock
15	Banja Luka Yugoslavia	Aug. 13 1981	La Villita, Guerrero Array	6.1	8.5	N90W	0.074	0.032	2.31	Rock

5.5 Scaling of Real Accelerograms

For the purpose of dynamic nonlinear analysis of a structure, the selected actual accelerograms should represent the level of the excitation motion expected at the location of the structure. Since the design spectrum specified by the code represents the level of the excitation (in addition to the frequency content), the selected actual accelerograms should be scaled in order to represent the code specified level. In this study, three different scaling approaches were used.

5.5.1 Scaling Based on Spectral Acceleration Ordinates

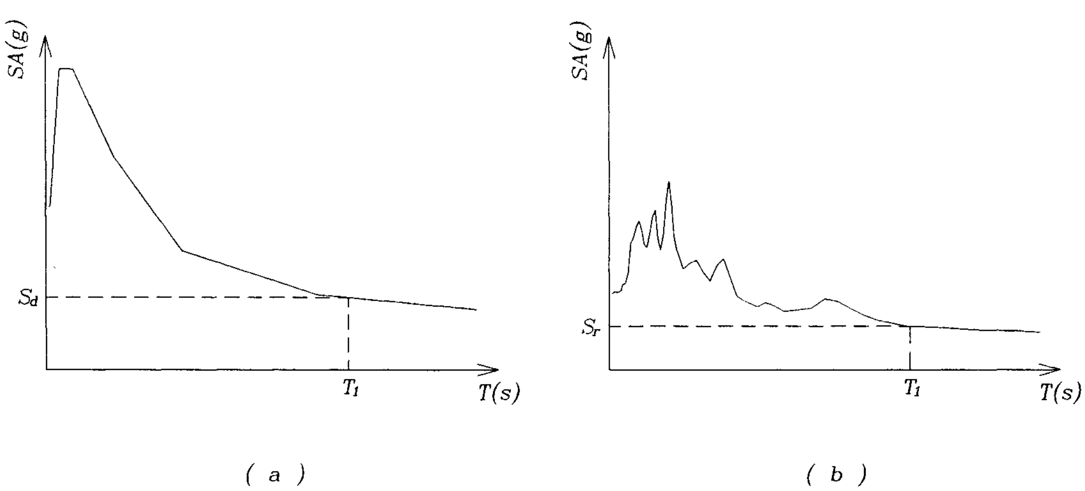

Fig. 5.5 Spectral acceleration ordinate as a scaling parameter; (a) design spectrum, (b) spectrum of real accelerogram

In this method, the accelerogram is scaled in such a way that the spectrum of the scaled accelerogram has the same ordinate as that of the design spectrum for the fundamental period of the structure. This type of scaling is illustrated in Fig. 5.5. The fundamental period of the structure is designated T_1 in the figure. If the ordinate of the design spectrum at the fundamental period, T_1, is designated as S_d, and that of the spectrum of the real accelerogram is designated S_r, then the scaling would consist of simply multiplication of the real accelerogram by the factor S_d/S_r. It should be mentioned that in this study, the fundamental period represents elastic period based on the gross sections of the members.

5.5.2 Scaling Based on Partial Area under Acceleration Spectrum Curve

The second type of scaling used in this study is based on the partial area under the spectral curves, i.e. between the second mode period (T_2) of the structure and 1.2 times the fundamental structural period, i.e. $1.2T_1$ (see Fig. 5.6). If the area between T_2 and $1.2T_1$ under the design spectrum is designated PA_d, and that under the spectrum of the actual accelerogram is designated PA_r, then the scaling would consist of multiplication of the actual accelerogram by the factor PA_d/PA_r.

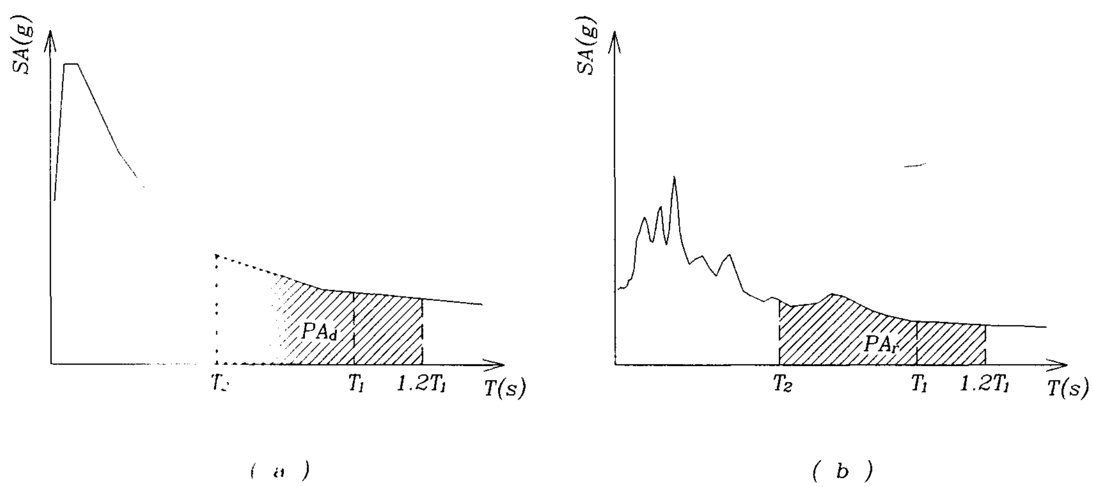

Fig. 5.6 Partial area under acceleration spectrum as a scaling parameter; (a) design spectrum, (b) spectrum of real accelerogram

5.5.3 Scaling Based on Full Area under Acceleration Spectrum Curve

In this type of scaling, the full area under the spectral curve of the actual accelerogram and that of the design spectrum between the periods of 0.02 s and 2.0 s is used as the scaling parameter (see Fig. 5.7). If the total area under the spectrum of the real accelerogram is designated FA_r, and that under the design spectrum is designated FA_d, then the scaling would consist of multiplication of the actual accelerogram by the factor FA_d/FA_r

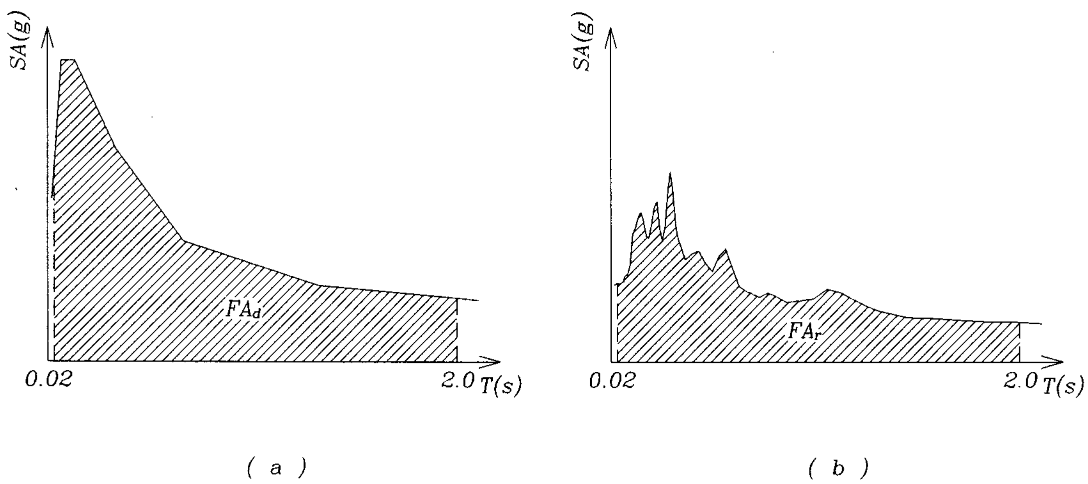

Fig. 5.7 Full area under acceleration spectrum as a scaling parameter; (a) design spectrum, (b) spectrum of real accelerogram

5.6 Summary for the Ensembles of Excitation Accelerograms Used in This Study

As discussed above, three major groups of accelerograms were used in this study as excitation motions in the analyses of the three buildings, i.e. (i) artificial accelerograms compatible with the design spectrum, (ii) simulated accelerograms using stochastic method, and (iii) real accelerograms that were scaled using three scaling methods (to spectral ordinate, to partial area under the spectral curve, and to full area under the spectral curve). The ensembles are summarized in Table 5.6. The table also shows which ensembles were used in the analysis of each building. It can be seen that all three buildings were analyzed using the artificial accelerograms compatible with the design spectra and the simulated accelerograms using stochastic method. In terms of the use of the real accelerograms, Building #1 was analyzed using the ensembles of real records for all three types of scaling (to spectral ordinate, to partial and full areas under the spectral curves). However it was found that the results from scaling to full area were somewhat larger than those from scaling to partial area. It was felt that the scaling to full area puts the same weight on the contributions of all the vibration modes, which is not the case for frame buildings. Given this, the ensembles from the scaling to full area were not used in the analysis of Buildings #2 and #3.

The mean spectra of the scaled ensembles of real records used in the analysis of the buildings, and the design spectra for Vancouver and Montreal are shown in Fig. 5.8. The mean spectra of the accelerograms compatible with the design spectra are practically the same as the design spectra throughout the whole period range. As can be seen from this figure, all three types of scaling provide relatively close mean spectra in the period range in the neighbourhood of the fundamental periods of the buildings (1.16 s for Buildings #1 and #2, and 1.13 s for Building #3).

Table 5.6 Summary of ensembles of accelerograms used in the analysis of the buildings

Ensemble name	Ensemble description	Reference sections	No. of time-histories in the ensemble	Building #1	Building #2	Building #3	City
ADCV	Artificial Design Compatible for Vancouver	5.2	15	✓	✓		Vancouver
RW-SO	Real records for West Scaled by Spectral Ordinate	5.3 5.5.1	15	✓	✓		Vancouver
RW-PA	Real records for West Scaled by Partial Area under spectrum curve	5.3 5.5.2	15	✓	✓		Vancouver
RW-FA	Real records for West Scaled by Full Area under spectrum curve	5.3 5.5.3	15	✓			Vancouver
M6.5R30	Simulated time-histories for west M6.5 R=30 km scenario	5.3	4	✓	✓		Vancouver
M7.2R70	Simulated time-histories for west M7.2 R=70 km scenario	5.3	4	✓	✓		Vancouver
ADCM	Artificial Design Compatible for Montreal	5.2	15			✓	Montreal
RE-SO	Real records for East scaled by Spectral Ordinate	5.3 5.5.1	15			✓	Montreal
RE-PA	Real records for East scaled by Partial Area under spectrum curve	5.3 5.5.2	15			✓	Montreal
M6.0R30	Simulated time-histories for east, M6.0 R=30 km scenario	5.3	4			✓	Montreal
M7.0R70	Simulated time-histories for east, M7.0 R=70 km scenario	5.3	4			✓	Montreal

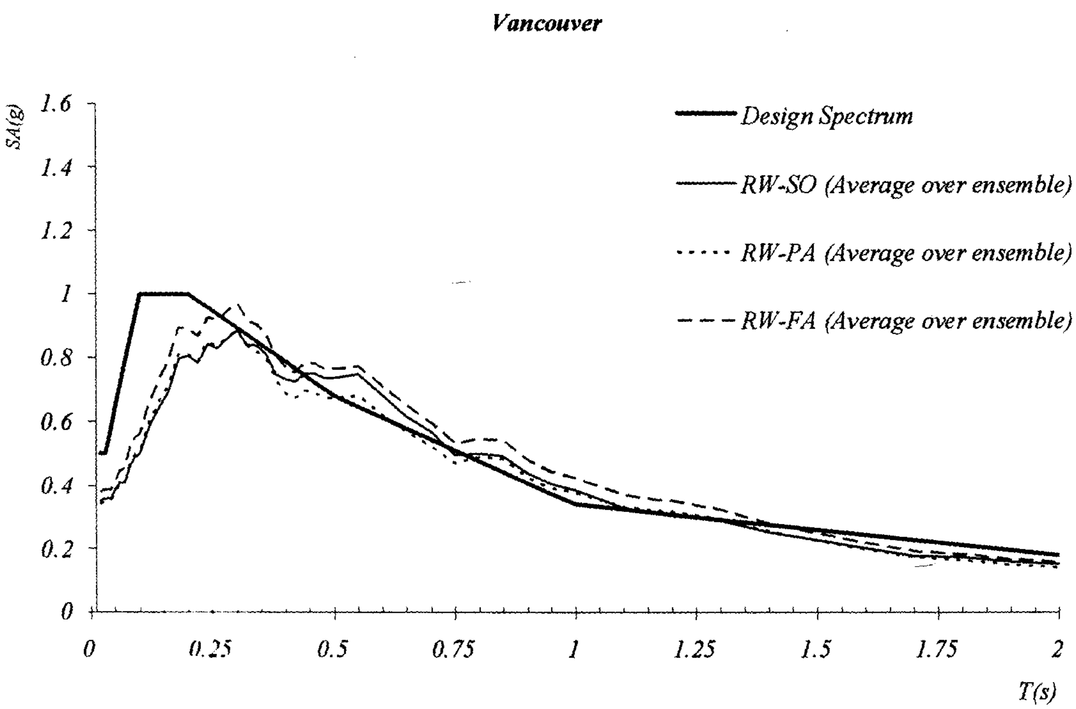

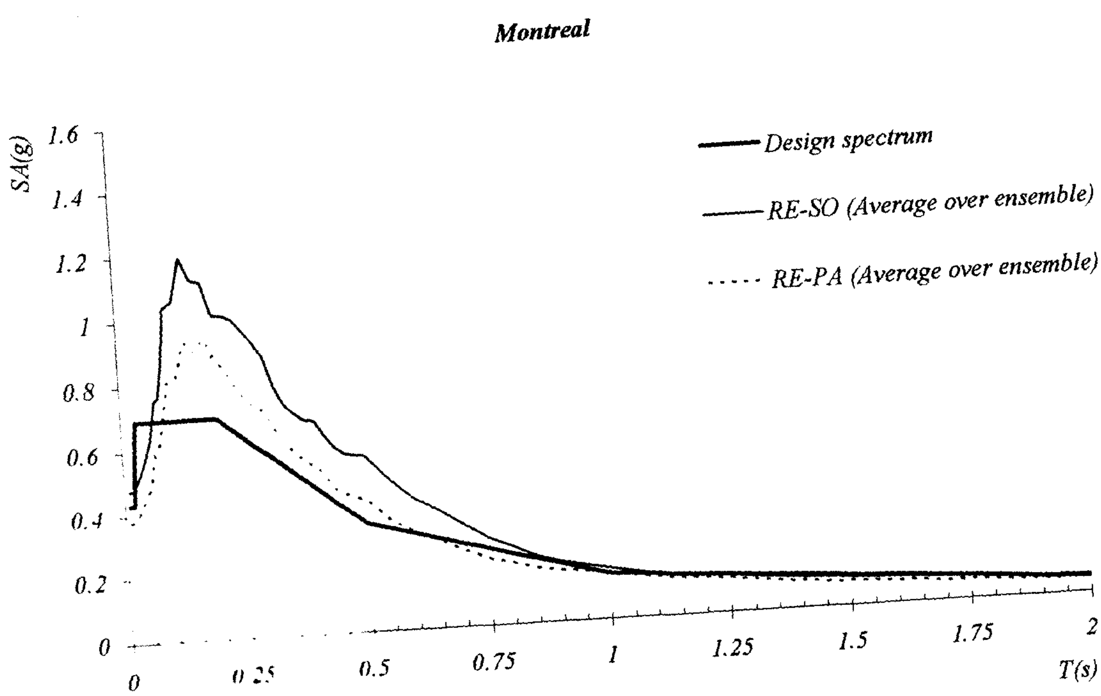

Fig. 5.8 Mean response spectra for scaled real records, and design spectra for Vancouver and Montreal

5.7 Two levels of excitation

The generated and the scaled real accelerograms as described above are assumed to represent the level of protection as required by the NBCC 2005. This level is referred to as "normal" level of excitation in this study. However, Heidebrecht (1995) has noted that earthquake motions as large as two to three times as those associated with the uniform hazard spectra (i.e., design spectra in NBCC 2005) can happen during the life time of the buildings. Given this, another intensity level of the excitation motions was used which was twice the normal level prescribed by the code, and will be referred to as "double" level of excitation. More details for these two excitation levels will be given in the next chapter.

CHAPTER 6

ANALYSIS AND RESULTS

6.1 Analysis and Response Parameters

For each building, nonlinear time-history analysis was conducted using the IDARC program by subjecting the building to each of the accelerograms of the ensembles listed in Table 5.6. This resulted in a total of 68 time-history analyses for Building #1, and 53 analyses for each of the Buildings #2 and #3. Both, the forced vibration and 10 seconds of free vibration (after the end of the earthquake accelerogram) were considered in each analysis. Two response parameters were used from the analyses, i.e. (i) interstorey drift, and (ii) curvature ductilities of the end sections of the beams and columns of the buildings. The interstorey drift represents a global response parameter of the seismic response of the structures. On the other hand, the curvature ductilities of the columns and beams represent local response parameters, and are indicators for the amount of inelastic deformations of the structural members. For the purpose of the evaluations of the scaling techniques on the response of the buildings, the response parameters of the buildings subjected to the records of the ensembles containing 15 accelerograms were statistically analyzed to compute the Mean (M) and Mean plus one Standard Deviation (M+SD) values. More details for the computation of the interstorey drifts and the curvature ductilities are presented hereafter.

6.1.1 Maximum Interstorey Drift

The interstorey drift is an important global parameter of the response of a given storey during seismic excitation. It is a relatively stable parameter, and it is used in building design codes to impose limits on the differential deflections of two consecutive floors. In the NBCC 2005, the maximum allowed interstorey drift is 2.5%. The program IDARC gives directly the maximum interstorey drift. It is computed from the differences of the lateral displacement time-histories of the floors, and is expressed as a percentage of the storey height.

6.1.2 Curvature Ductility Demand

The IDARC program provides time-histories of moments and curvatures for both end sections of each structural member. Using these time-histories, one can plot the hysteretic loops. An example of such a plot is given in Fig. 6.1.

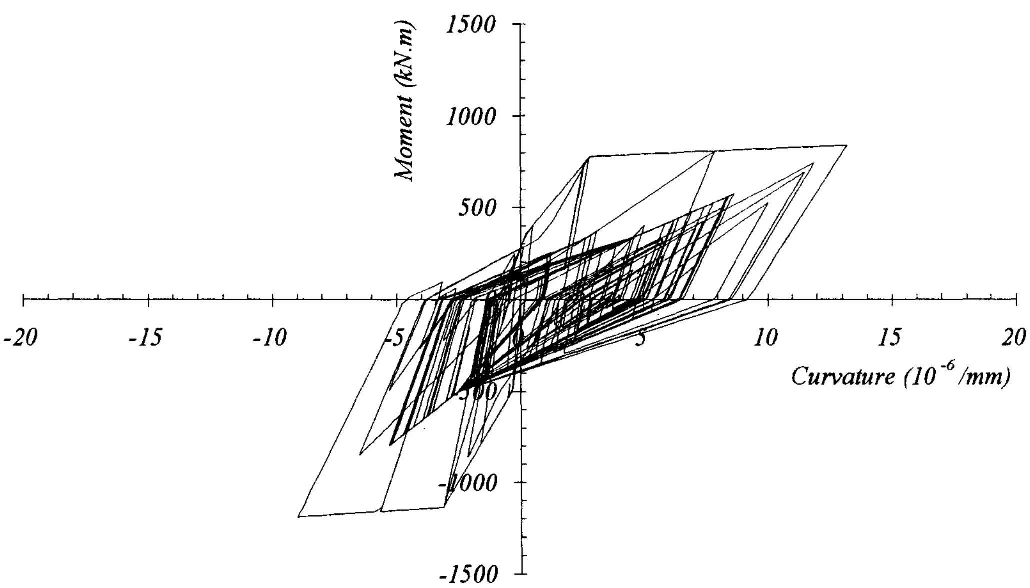

Fig. 6.1 Moment-curvature hysteretic loops for a beam section of the fifth floor of Building #1, subjected to accelerogram No. 2 from the ADCV ensemble (Artificial Design Compatible for Vancouver), double level of excitation.

Positive curvature ductility demand was then calculated as the ratio of the maximum positive response curvature to the positive yield curvature of the section; for a given section of a structural member, maximum positive response curvature was computed from the curvature response time-history provided by IDARC, and the positive yield curvature capacity was taken from the tri-linear moment-curvature envelope for that section which was used as an input in IDARC (see Chapter 4 for discussion of the tri-linear moment-curvature envelopes). The computation of the negative curvature ductility demand was conducted in the same way, but using the negative curvature response and the negative yield curvature capacity of the section. For a given section, the larger of the absolute values of the positive and negative ductility demands was used as the maximum curvature ductility demand for that section.

6.2 Discussion of Results

Given the large number of time-history analyses, and also the large number of structural members in each of the buildings, the analysis of the response interstorey drifts and curvature ductility demands by considering all the results from each time-history analysis is impractical. Therefore, the drifts and the ductilities were statistically analyzed to compute their Mean (M) and Mean plus one Standard Deviation (M+SD) values. This was done for each of the ensembles of excitation motions containing 15 accelerograms. For each of these ensembles, mean and M+SD values were computed for the interstorey drifts, and these values were used in the evaluation of the effects of the scaling of the excitations on the interstorey drift.

In terms of the curvature ductility demands, the amount of mean and M+SD data is much larger than those of interstorey drifts. Namely, there are 8 mean values for columns and 6 mean values for beams, and the same number of M+SD values for each storey of building #3. As for Buildings #1 and #2, these numbers are raised to 12 for columns and 10 for beams of each storey. Therefore, for a given storey, only the maximum values of the mean and the M+SD curvature ductilities for the columns were used. Similarly, for a given floor, only the largest mean and M+SD curvature ductilities for the beams were considered. As an example, Fig. 6.2 illustrates the mean values of responses from the RW-SO (Real records for West, scaled to Spectral Ordinate) ensemble, normal level of excitation, for Building #1.

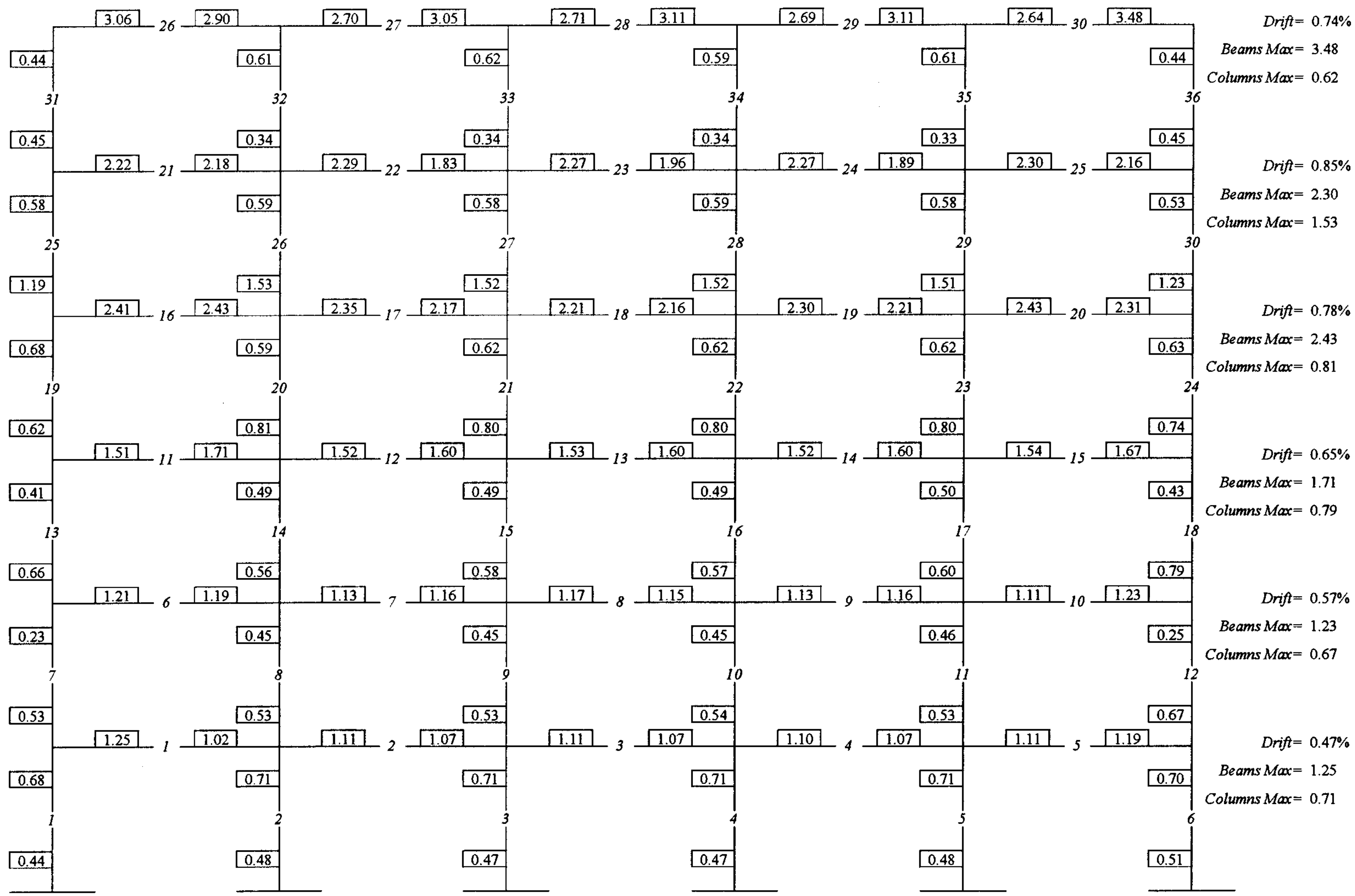

Fig. 6.2 Mean of responses from the RW-SO (Real records for West, scaled to Spectral Ordinate) ensemble, normal level of excitation, Building #1.

Curvature ductility demands printed at each end of beams and columns are the mean of all 15 values at that specific section, then, maximum of mean values of each floor are also shown separately for beams and columns. Displayed values for drifts are the mean values of all 15 drift values at the storey.

As mentioned earlier, no statistical analyses were conducted for the response parameters resulting from the simulated stochastic ensembles. This was because each of these ensembles contains only 4 accelerograms, which is not sufficient for any statistical analysis. The maximum interstorey drifts and the curvature ductility demands associated with each accelerogram of the simulated stochastic ensembles were considered separately. Therefore, the storey maximum for curvature ductilities is found among the responses for every accelerogram and not among the mean or M+SD values.

All the results are presented in Fig. 6.3 to Fig. 6.20. For each ensemble of 15 accelerograms, the right-hand end of the horizontal bar shows the mean value for each storey. The bar is then continued further to the right by a thin line. The right-hand end of the thin line is marked with a perpendicular small thick which shows the M+SD value. The mean and M+SD values are also given in front of each bar along with the ensemble name.

For each of the simulated stochastic ensembles, all four values are marked with points. Values of responses corresponding to the four points are given along with the ensemble name.

6.2.1 Results for Building #1, Normal Level of Excitation

The results for Building #1 when subjected to the ensembles described earlier are shown in Fig. 6.3 to Fig. 6.5. Considering the design spectrum compatible ensemble, ADCV (which is prescribed by the draft version of NBCC 2005) as a reference case, the figures show that the real records (for western Canada, designated RW) scaled either to spectral ordinate (RW-SO), or to partial area (RW-PA) give responses that are very close to the reference case, especially for the mean values. The ratios of the maximum to the minimum mean response values for the ADCV, RW-SO and RW-PA ensembles are as between 1.02 and 1.14 for interstorey drifts, between 1.04 and 1.28 for beam curvature ductilities, and between 1.06 and 1.28 for column ductilities. In some cases, the results from the scaling to full area give slightly larger responses than the other cases. This observation can be explained by considering the spectra shown in Fig. 5.8. This figure shows that the mean response spectrum for the scaling based on full area is somewhat higher than spectra from the scaling based on spectral ordinate or partial area. On the other hand, the spectra from the scaling based on spectral ordinate and partial area are quite close to the design spectrum for Vancouver within the period range in the neighbourhood of the fundamental period of the building (i.e., 1.16s).

The responses due to the simulated stochastic accelerograms show quite different features. For the M6.5R30 ensemble, all four responses are significantly larger than even the M+SD values of the artificial and the scaled real ensembles except for the two top floors. This can be explained by considering Fig. 5.3 (for Vancouver). As shown in this figure, the M6.5R30 response spectra are much higher than the design spectrum for Vancouver, especially in the neighbourhood of the fundamental period of the building (i.e., 1.16s). Since the simulated stochastic records are not compatible with the design spectrum for Vancouver, the further discussion will be mainly focused on the results of the other ensembles (i.e., the artificial accelerograms compatible with the design spectrum, and the scaled real accelerograms).

Among the three ensembles of interest (i.e., ADCV, RW-SO and RW-PA), the following results are observed: The drifts are well below the code limit of 2.5%. The maximum M+SD interstorey drift is 1.17% at the fifth storey. The maximum M+SD ductility in the beams is 5.20, and the maximum mean value is 3.61, both happening at the sixth floor. Except for the 5^{th} floor, where the maximum M+SD column ductility is 3.01, the ductilities of the columns at other storeys are mostly below 1.0 (i.e., no yielding occurs in the columns). In general, these curvature ductilities are not significant, since the members of well designed ductile moment-resisting frame can sustain curvature ductilities of 10 to 20 (Heidebrecht and Naumoski 2002).

Since the building was designed as a ductile frame, one would expect to obtain much larger ductilities in both the columns and the beams. The relatively small ductility values that were obtained from the analyses raise the question on the reasons for such results.

There are two major reasons for that. First, a conservatism is involved in the design of the structural members of the frames through the use of material resistance factors of Φ_c=0.6 and Φ_s=0.85 for concrete and reinforcing steel respectively. However, the most important reason is associated with the period used in the design of the building.

As it was stated in 3.1, this building was originally designed for the fundamental period of 0.6 s and a lateral force equal to 6.62% of the overall weight of the building. Assuming a design in compliance with NBCC 2005 with fundamental period of 0.84 s would lead to a base shear of 6.60% of total weight as lateral base shear (see Section 3.1 and Table 3.1). On the other hand, performing dynamic analysis makes the building respond at its actual period which is 1.16s. Recalculation of V/W in Table 3.1 for a period of 1.16 s according to NBCC 2005 would yield V/W=4.62%. This means that the lateral force coefficient for which the building is designed (i.e., 6.62%) is 43% larger than the virtual lateral force coefficient for which the building is actually analyzed (i.e., 4.62%). This extra 43% becomes even more important considering the fact that, carrying half of the building for lateral forces, the frame under consideration is dominated by lateral force rather than gravity loads (see 3.1).

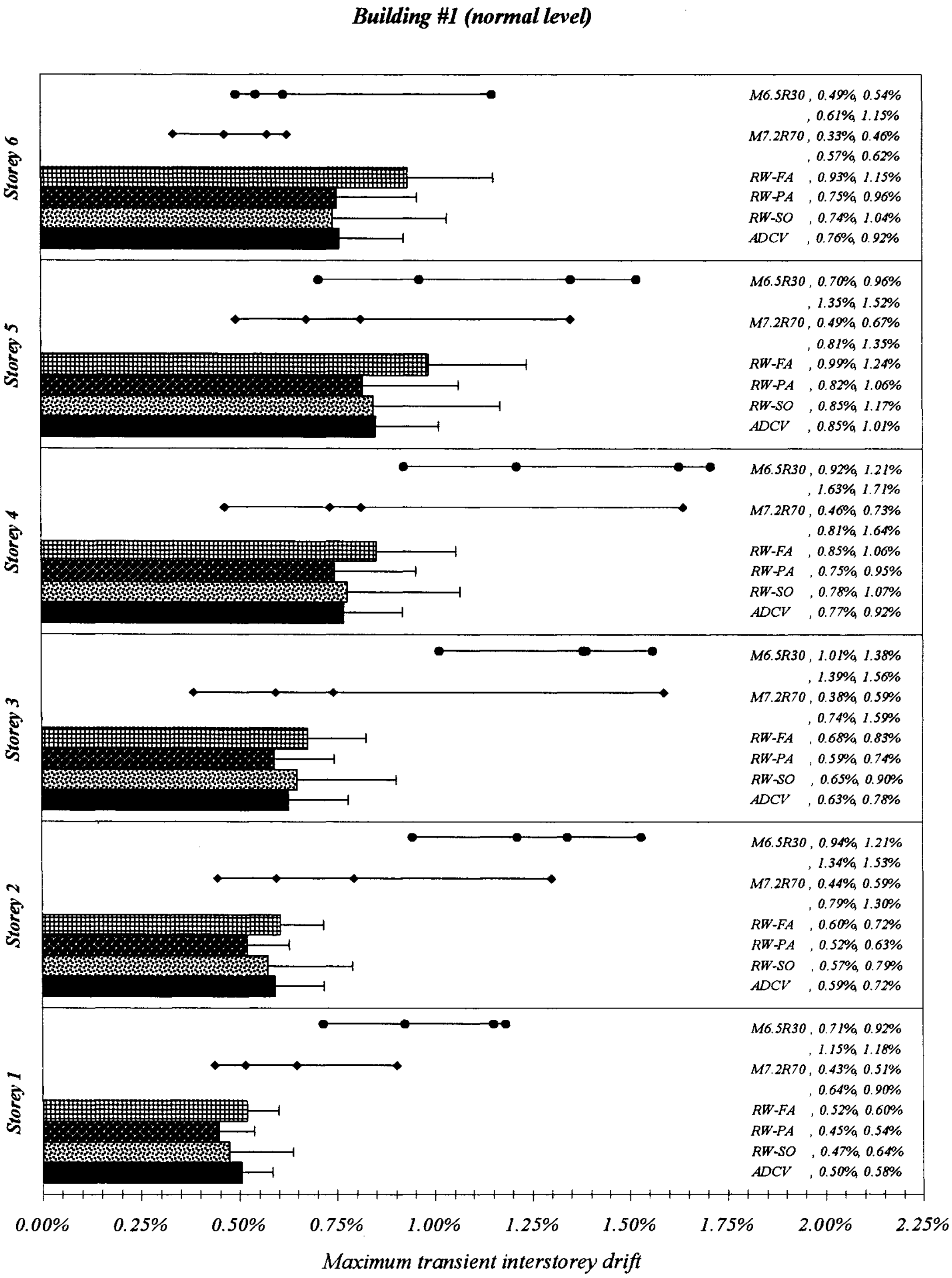

Fig. 6.3 Maximum transient interstorey drift, Building #1, normal level of excitation.

Mean and M+SD values are presented for the ensembles of 15 accelerograms. The values for each of the four accelerograms of the simulated ensembles are presented.

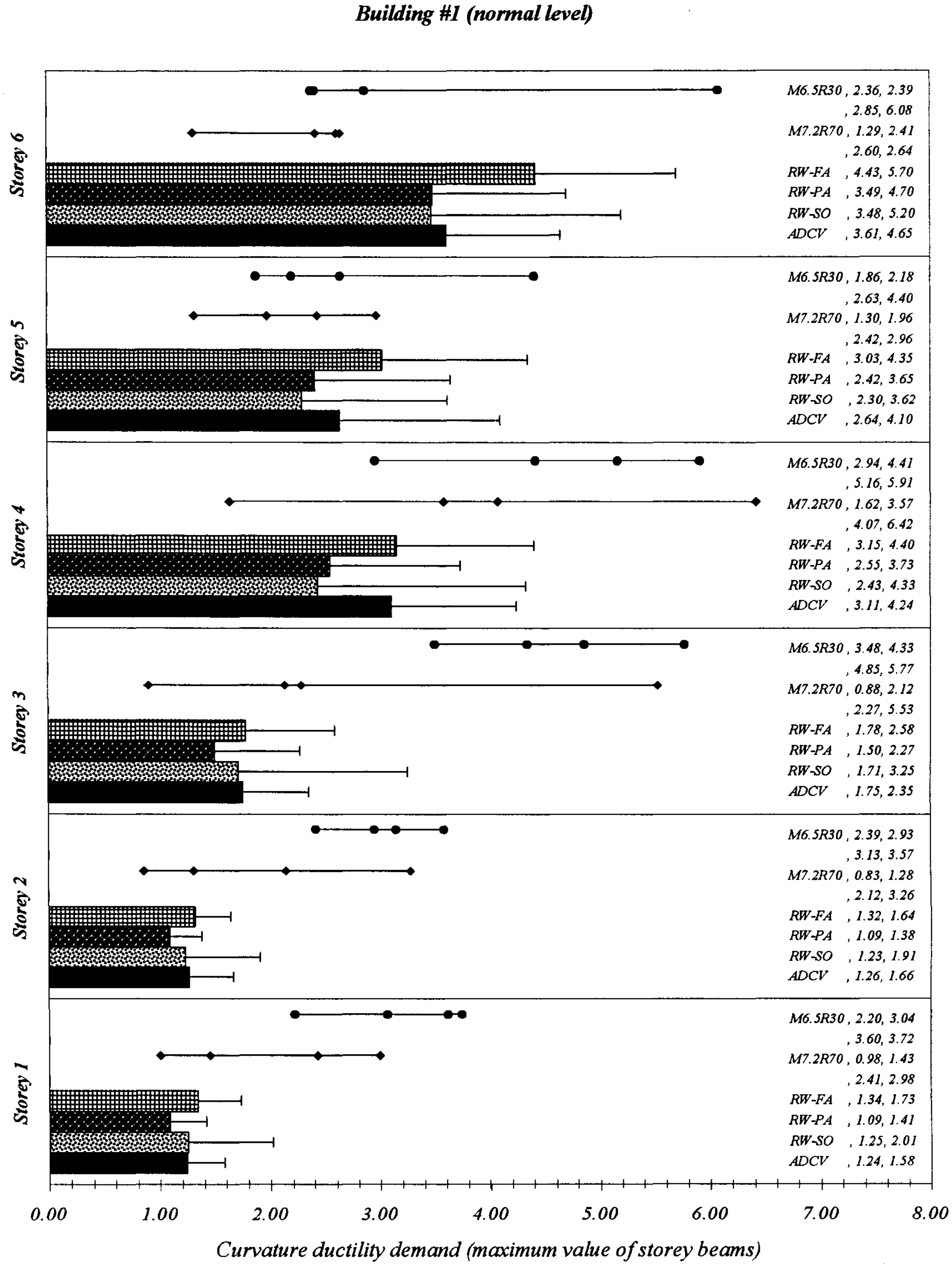

Fig. 6.4 Beam curvature ductility demands, Building #1, normal level of excitation.

Maximum values of the mean and M+SD ductilities at each floor are presented for the ensembles of 15 accelerograms. The values for each of the four accelerograms of the simulated ensembles are shown.

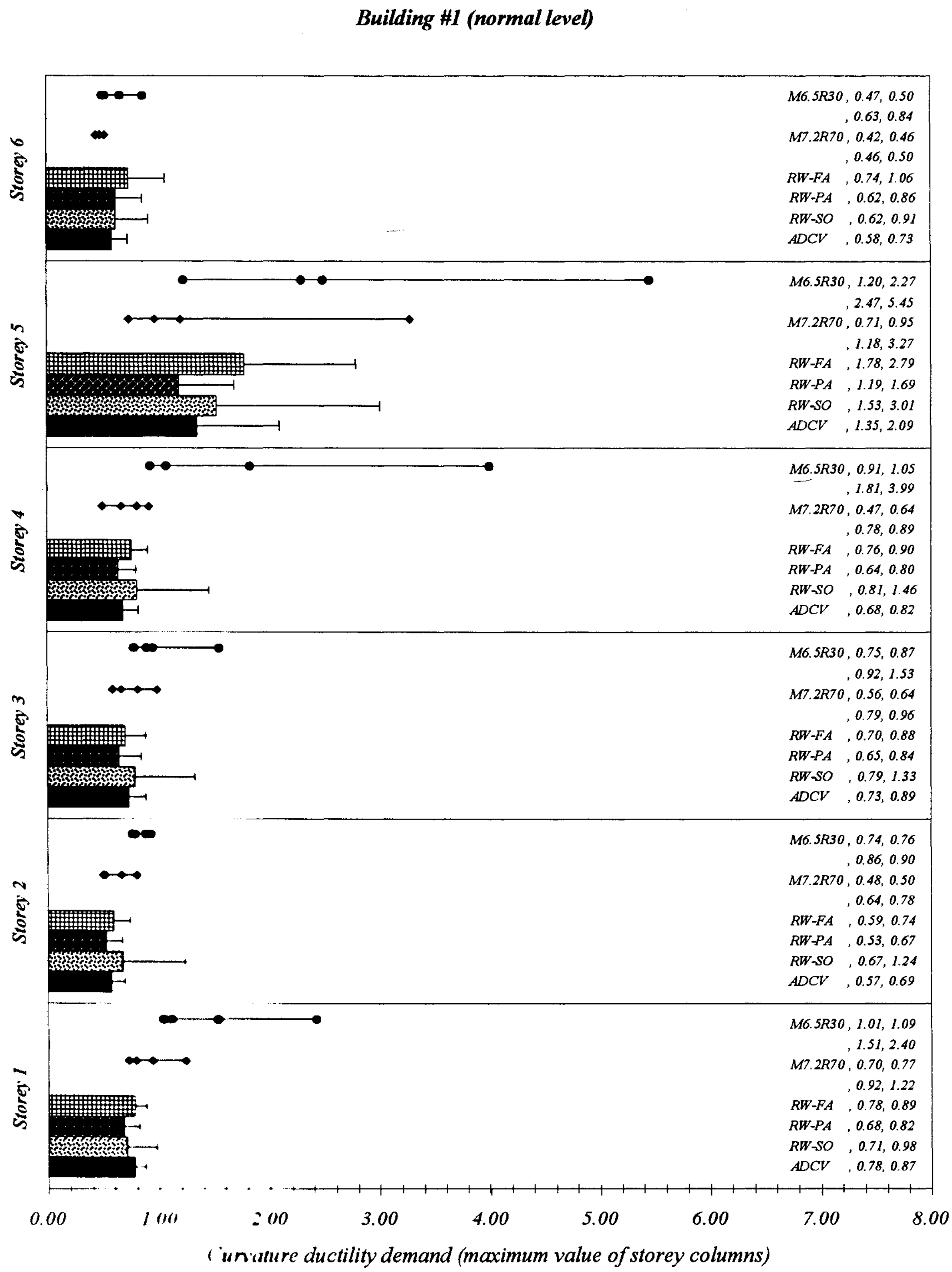

Fig. 6.5 Column curvature ductility demands, Building #1, normal level of excitation.

Maximum values of the mean and M+SD ductilities at each floor are presented for the ensembles of 15 accelerograms. The values for each of the four accelerograms of the simulated ensembles are shown.

6.2.2 Results for Building #1, Double Level of Excitation

The results for Building #1 when subjected to the double level of excitation are shown in Fig. 6.6 to Fig. 6.8. At first glance, the trend of the results from the double level of the different excitation ensembles is seen to follow the trend of the results from the normal level of the ensembles. Thus, responses from the ADCV (Artificial Design spectrum Compatible accelerograms for Vancouver), the RW-SO (Real accelerograms for West scaled to Spectral Ordinate) ensemble, and the RW-PA (Real accelerograms for West Scaled to Partial area under the spectrum) ensemble, are relatively comparable. The ratios of the maximum to the minimum values of the mean responses of these three ensembles are between 1.02 and 1.20 for interstorey drifts, between 1.07 and 1.30 for beam curvature ductilities, and between 1.05 and 1.38 for column ductilities. The responses resulting from the ensemble of real records for western Canada scaled to full area under the spectral curve (designated RW-FA) are generally slightly larger than the values of the ADCV, RW-SO, and RW-PA ensembles, as was the case for the normal level of excitation. Also, the simulated accelerograms produce larger responses than those of the other four ensembles (i.e., ADCV, RW-SO, RW-PA, and RW-FA), as was observed from the normal level of excitation. The reasons for obtaining larger values from the RW-FA and the simulated ensembles were discussed in section 6.2.1. Given these differences, our focus is mainly on the results from the ensembles ADCV, RW-SO and RW-PA which provide relatively comparable responses (as was the case for the normal level of excitation).

Among the three ensembles of interest (i.e., ADCV, RW-SO and RW-PA), the following results are observed: The mean values of interstorey drifts are mostly below the code limit of 2.5%, with the exception of the fifth storey where the drift is 2.97%, this is slightly above the code limit. The maximum value of the M+SD interstorey drift is 4.41%. This is also at the fifth storey. The maximum values of the beam curvature ductilities at the mean and M+SD levels are 11.84 and 18.09 respectively. In terms of the column ductilities, the maximum values at the mean and M+SD deviation levels are 6.54 and 9.95 respectively; both of these values are for the columns of the fifth storey. The column ductilities for the other storeys are much smaller, i.e., below 2.38 at the mean level and below 4.84 at the M+SD level.

The results for the double excitation level (Fig. 6.6 to Fig. 6.8), as discussed above, were not surprising. As reported in Heidebrecht and Naumoski (2002), well designed ductile reinforced concrete frame building can sustain curvature ductilities of the order of 15 to 20. It is important to note that the largest ductilities are in the beams, as expected, and those in the columns are much smaller.

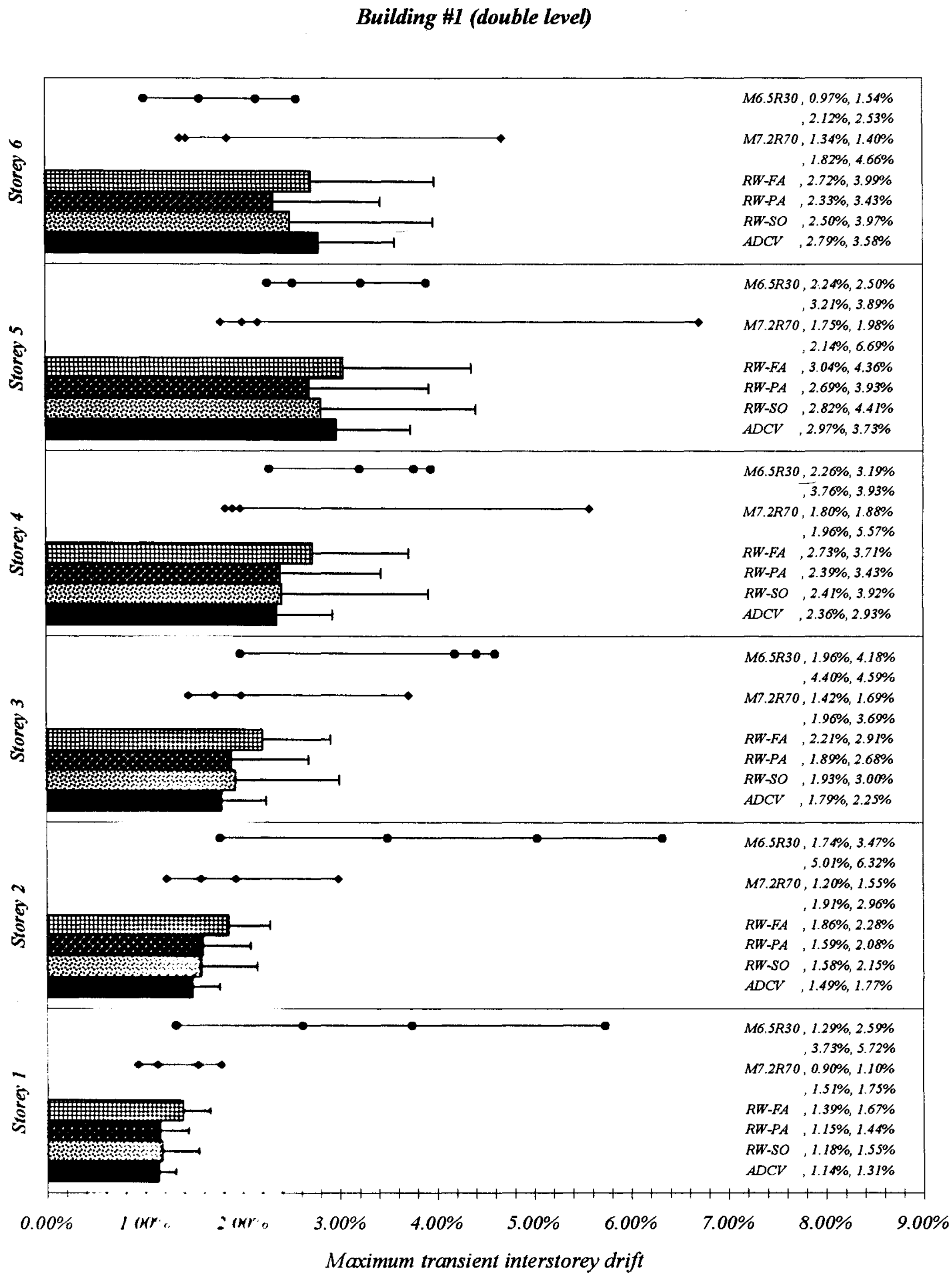

Fig. 6.6 Maximum transient interstorey drift, Building #1, double level of excitation.

Mean and M+SD values are presented for the ensembles of 15 accelerograms. The values for each of the four accelerograms of the simulated ensembles are presented.

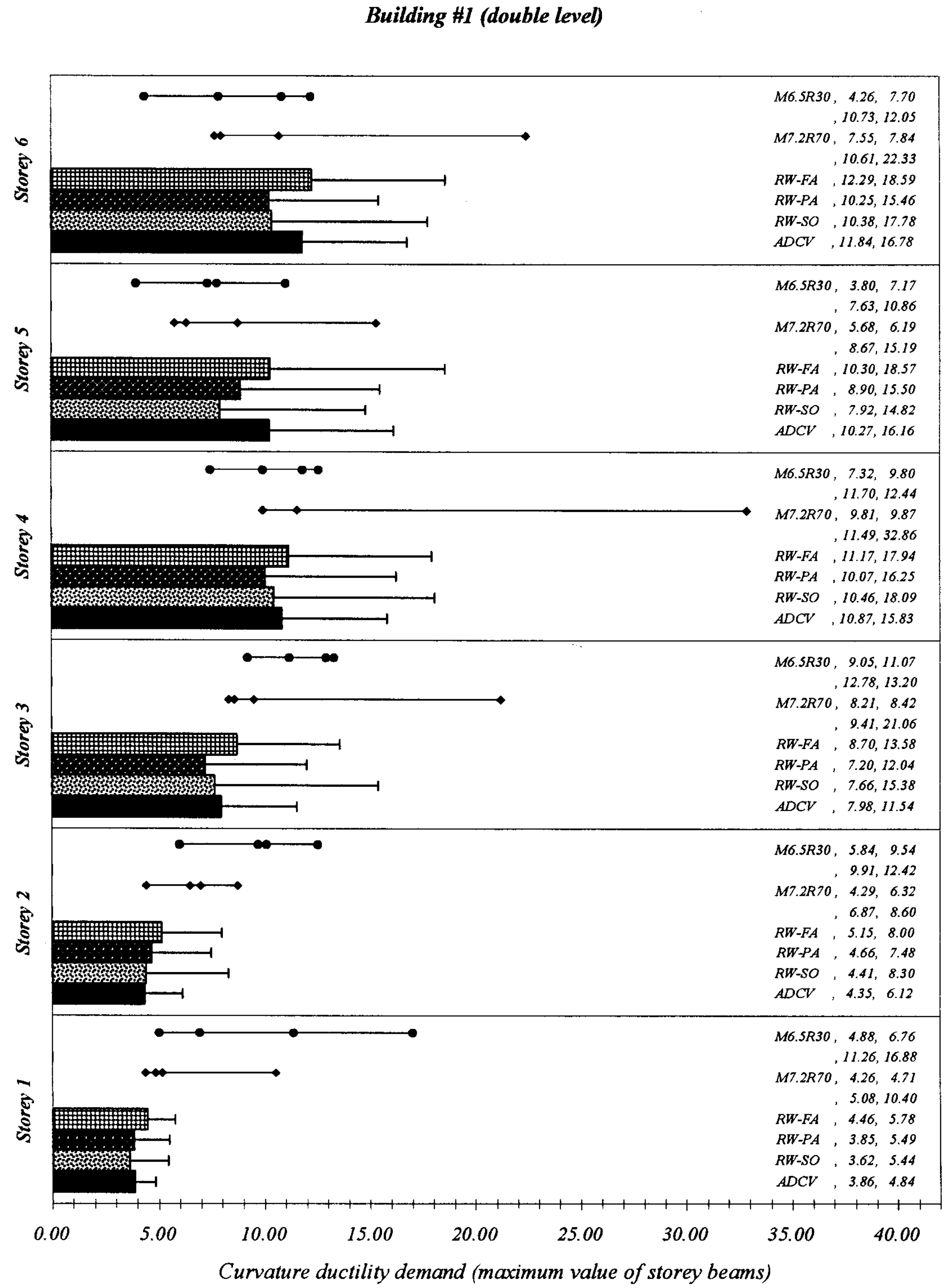

Fig. 6.7 Beam curvature ductility demands, Building #1, double level of excitation.

Maximum values of the mean and M+SD ductilities at each floor are presented for the ensembles of 15 accelerograms. The values for each of the four accelerograms of the simulated ensembles are shown.

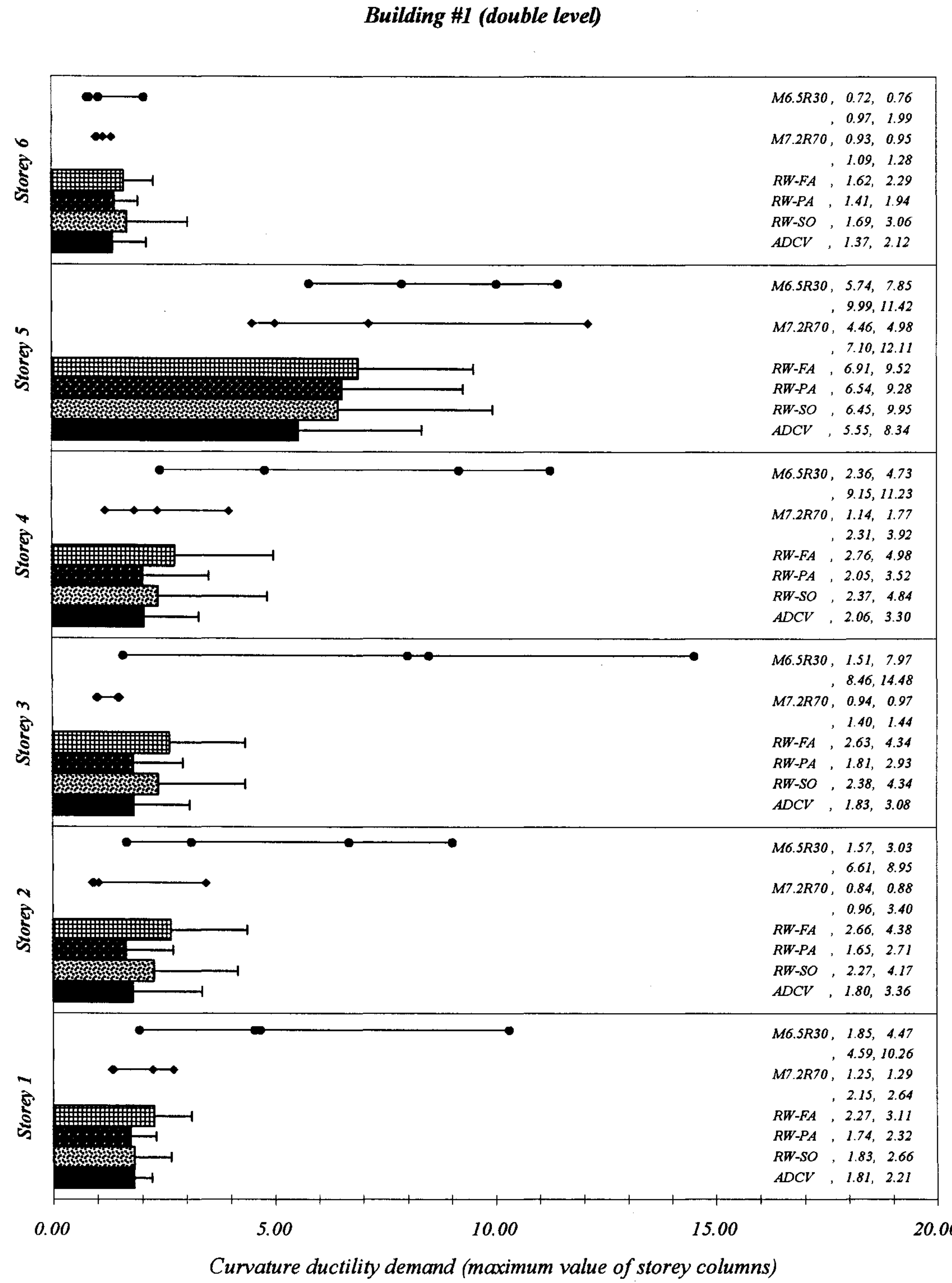

Fig. 6.8 Column curvature ductility demands, Building #1, double level of excitation.

Maximum values of the mean and M+SD ductilities at each floor are presented for the ensembles of 15 accelerograms. The values for each of the four accelerograms of the simulated ensembles are shown.

6.2.3 Results for Building #2, Normal Level of Excitation

The results for Building #2, for the normal level of excitation are shown in Fig. 6.9 to Fig. 6.11. As discussed earlier, the frames of this building were designed as nominally ductile frames (i.e., using force reduction factor of 2 according to NBCC 1995). Based on the results for Building #1, the ensemble of real accelerograms scaled to full area under the spectral curves (i.e., RW-FA ensemble) was not used in the analyses of Building #2. As mentioned earlier, the responses due to this ensemble are somewhat larger than those of the other three ensembles (i.e., ADCV, RW-SO and RW-PA ensembles); primarily because the mean spectrum of this ensemble is somewhat higher than those of the other ensembles in the neighbourhood of the fundamental period of the building (see Fig. 5.8). Also, the responses due to the simulated accelerograms are much larger than those from the ensembles ADCV, RW-SO and RW-PA, because these accelerograms are not compatible with the design spectrum for periods around the fundamental period of the building (see Fig. 5.3). Given this, the further discussion of the results will be focused on those from the ensembles ADCV, RW-SO and RW-PA.

As shown in Fig. 6.9, the mean interstorey drifts resulting from the three ensembles with 15 accelerograms (ADCV - Artificial Design spectrum Compatible accelerograms for Vancouver, RW-SO – Real accelerograms for West scaled to Spectral Ordinate, and RW-PA – Real accelerograms for West scaled to Partial Area under the spectral curve) are quite close for all six storeys of the building. In terms of the mean interstorey drifts, the ratios of the maximum to the minimum mean values (at each storey) among the three ensembles range from 1.03 to 1.17. The maximum values of the interstorey drifts at the mean and the M+SD levels are 0.75% and 1.17% respectively. These values are very close to those of Building #1.

In terms of the curvature ductilities of the beams, Fig. 6.10 shows that the maximum ductility values at the mean and the M+SD levels are 3.02 and 6.41 respectively. Both these values are at the sixth floor (i.e., the roof), and the values for the other floors are much smaller. At each floor, the ratios of the maximum to the minimum ductility values at the mean level among these three ensembles range between 1.07 and 1.30.

The trend of the column ductilities is similar to that of the beams. The largest values are at the sixth storey. The maximum ductilities at the mean and M+SD level are 1.65 and 2.66 respectively. Both these values are at the sixth storey, and the values for the other storeys are much smaller (see Fig. 6.11). The ductilities from the three ensembles are quite close. The ratios of the maximum to the minimum mean values (at each storey) among the three ensembles range between 1.02 and 1.19.

In a summary, the overall response of the building does not show large inelastic deformations. This is primarily because the building was designed as nominally ductile frame, for which the design base shear is two times that used in the design of Building #1. The other reasons for such behaviour are the same as those discussed for Building #1 in section 6.2.1. It is useful to mention again here that the building was designed for a fundamental period of 0.6 s, according to the NBCC 1995 formula, and a lateral force of 13.25% of the overall weight of the building (see Table 3.3). On the other hand, the response of the building in the dynamic analysis corresponds to the actual period of 1.16 s. For this period, the lateral base shear is 8.98% of the overall weight of the building. This means that the design base shear is about 48% larger than that corresponding to the actual period of 1.16 s.

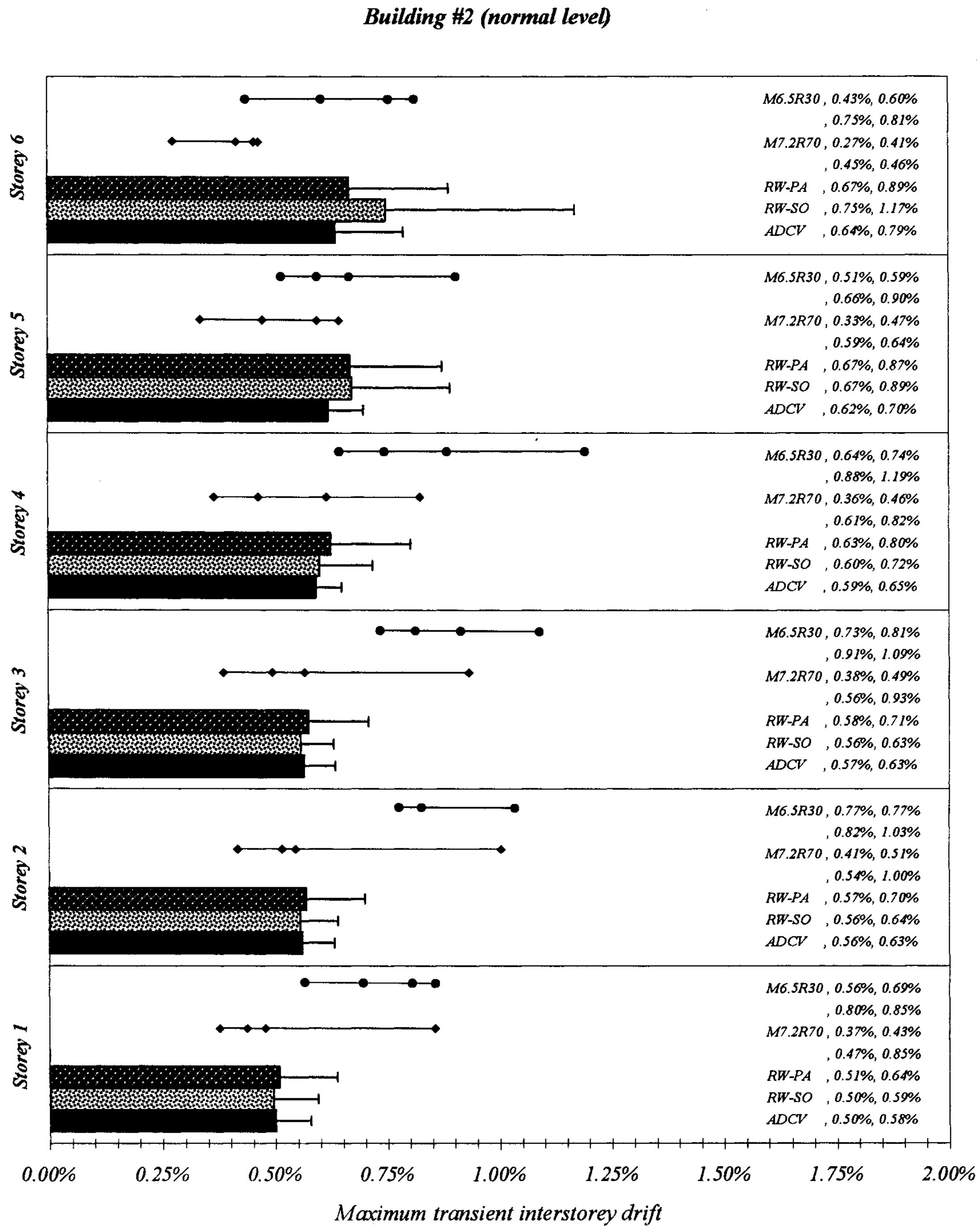

Fig. 6.9 Maximum transient interstorey drift, Building #2, normal level of excitation.

Mean and M+SD values are presented for the ensembles of 15 accelerograms. The values for each of the four accelerograms of the simulated ensembles are presented.

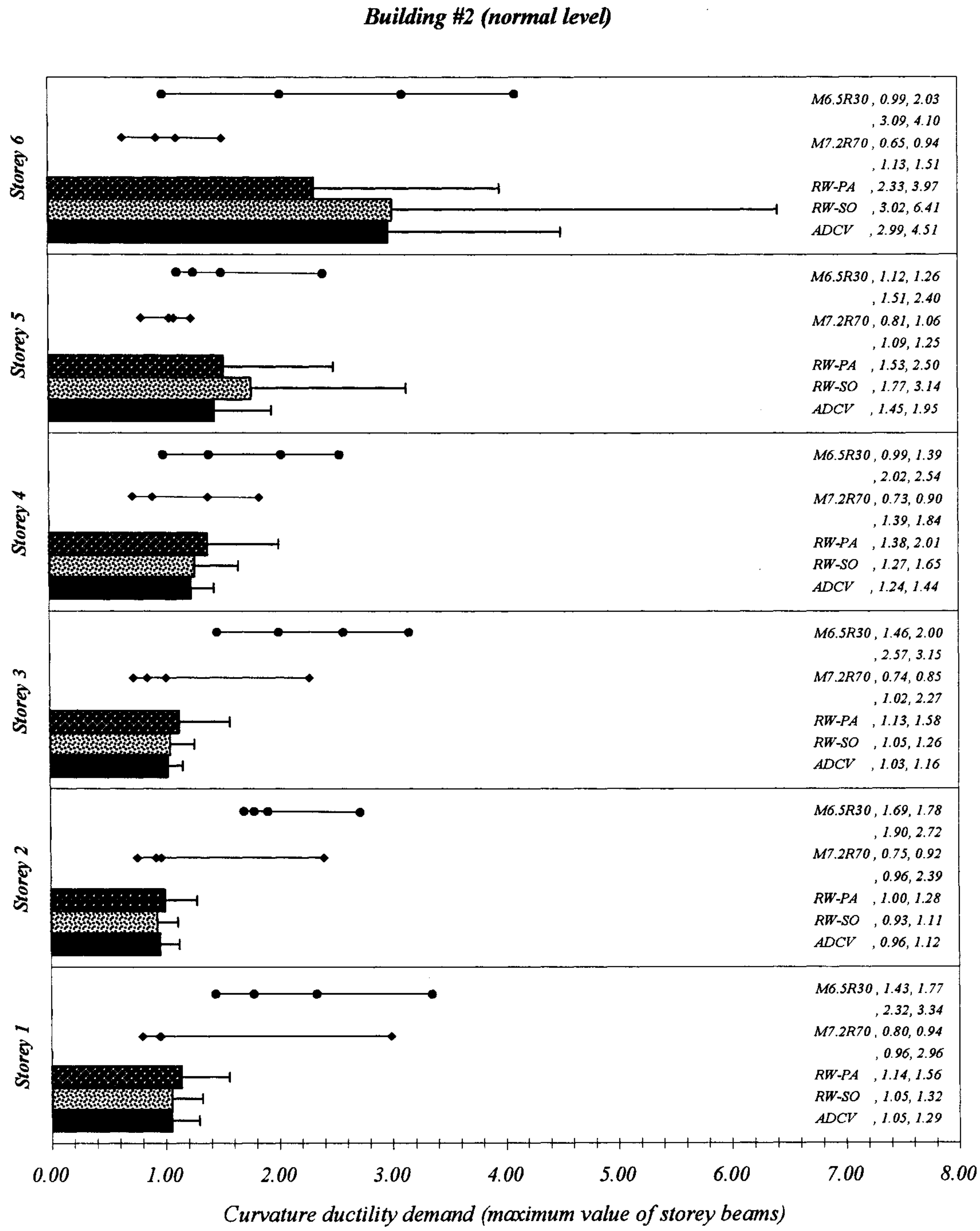

Fig. 6.10 Beam curvature ductility demands, Building #2, normal level of excitation.

Maximum values of the mean and M+SD ductilities at each floor are presented for the ensembles of 15 accelerograms. The values for each of the four accelerograms of the simulated ensembles are shown.

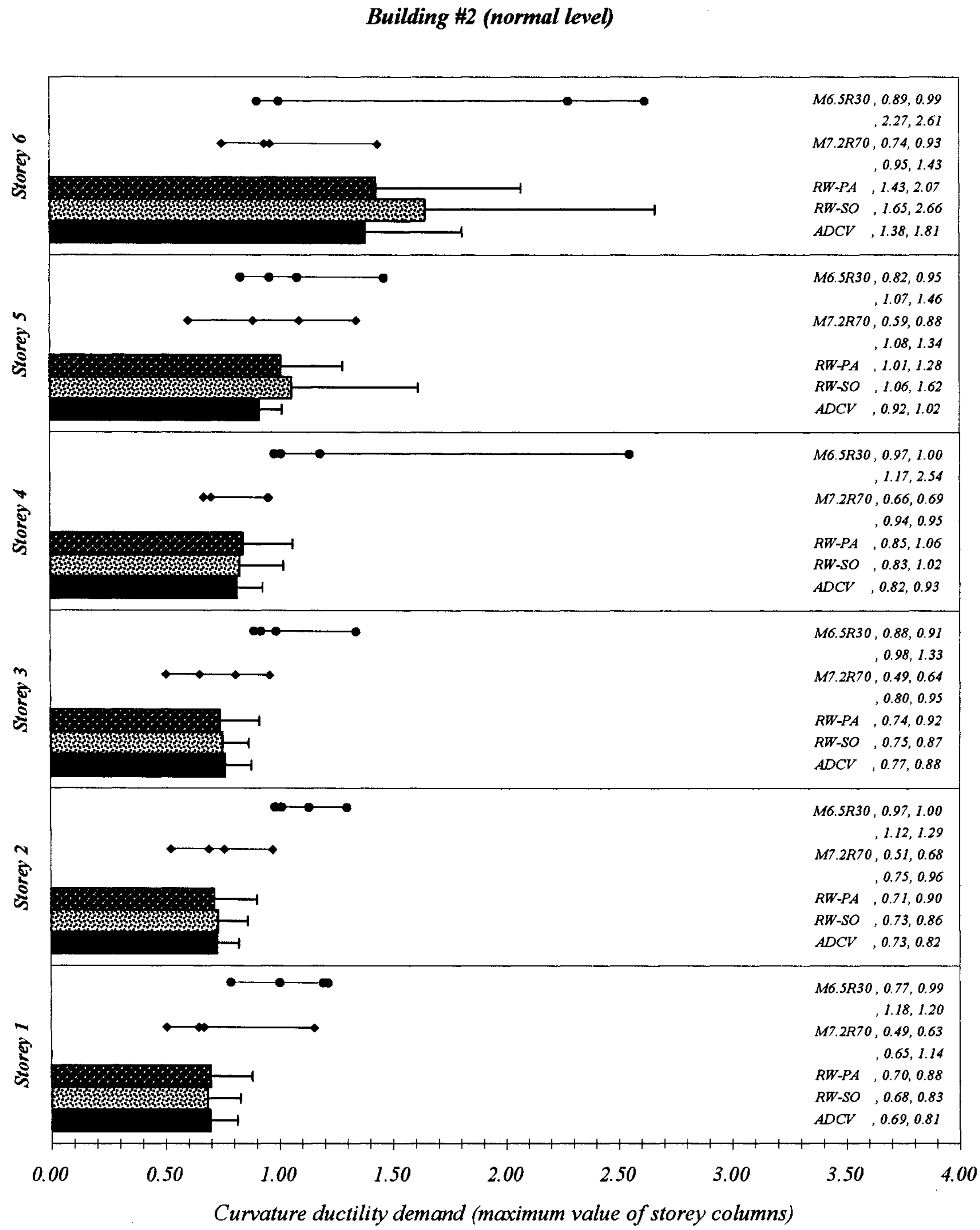

Fig. 6.11 Column curvature ductility demands, Building #2, normal level of excitation.

Maximum values of the mean and M+SD ductilities at each floor are presented for the ensembles of 15 accelerograms. The values for each of the four accelerograms of the simulated ensembles are shown.

6.2.4 Results for Building #2, Double Level of Excitation

The results for Building #2 for the double level of excitation are shown in Fig. 6.12 to Fig. 6.14. Again, these figures show that the results from the three ensembles with 15 accelerograms (i.e., ADCV, RW-SO and RW-PA) are quite comparable. Responses from the simulated accelerograms are significantly larger than those of the other ensembles. As in the previous cases, the discussion will be mainly focused on the responses resulting from the three ensembles of 15 accelerograms.

As shown in Fig. 6.12, the maximum values of the interstorey drifts at the mean and M+SD levels are 2.70% and 3.76% respectively; both these values are at the sixth storey. The drifts resulting from the three ensembles are quite close, especially for the mean level. The ratios of the maximum to the minimum mean drift values (for each storey) among the three ensembles range between 1.04 and 1.16.

In terms of the curvature ductilities in the beams, the maximum values at the mean and M+SD levels are 18.00 and 25.47 respectively. These values are at the sixth storey (i.e., at the roof level). The beam ductilities at the other floors are much smaller, i.e., the mean and M+SD values are all below 8.81 and 13.30 respectively. The ratios of the maximum to the minimum mean beam ductility values (at each floor level) among the three ensembles are in the range between 1.08 and 1.51.

The column ductilities (Fig. 6.14) are much smaller than the beam ductilities. The maximum column ductilities at the mean and M+SD levels are 3.11 and 4.58 respectively. The ratios of the maximum to the minimum mean column ductilities (at each storey) among the three ensembles are between 1.11 and 1.25.

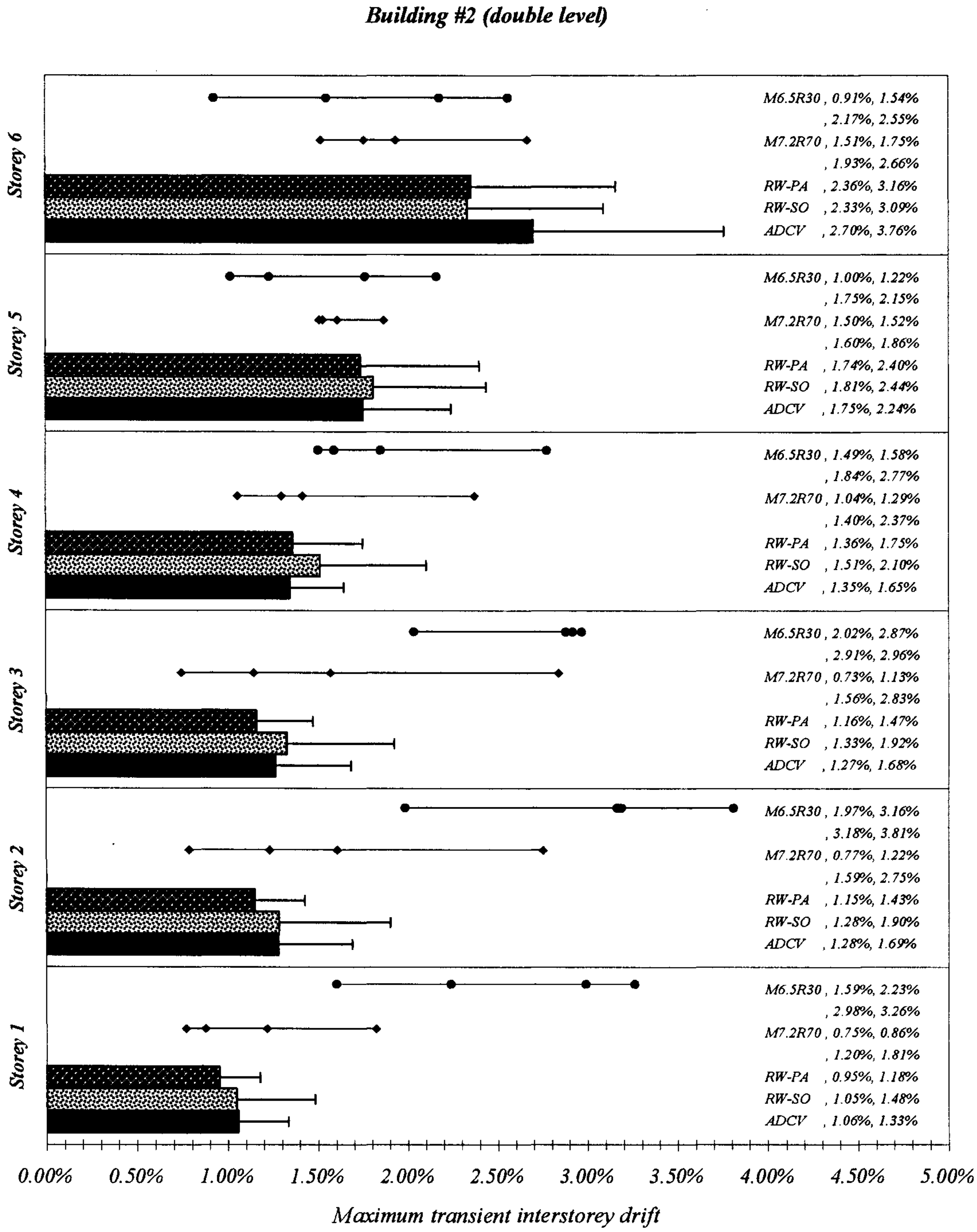

Fig. 6.12 Maximum transient interstorey drift, Building #2, double level of excitation.

Mean and M+SD values are presented for the ensembles of 15 accelerograms. The values for each of the four accelerograms of the simulated ensembles are presented.

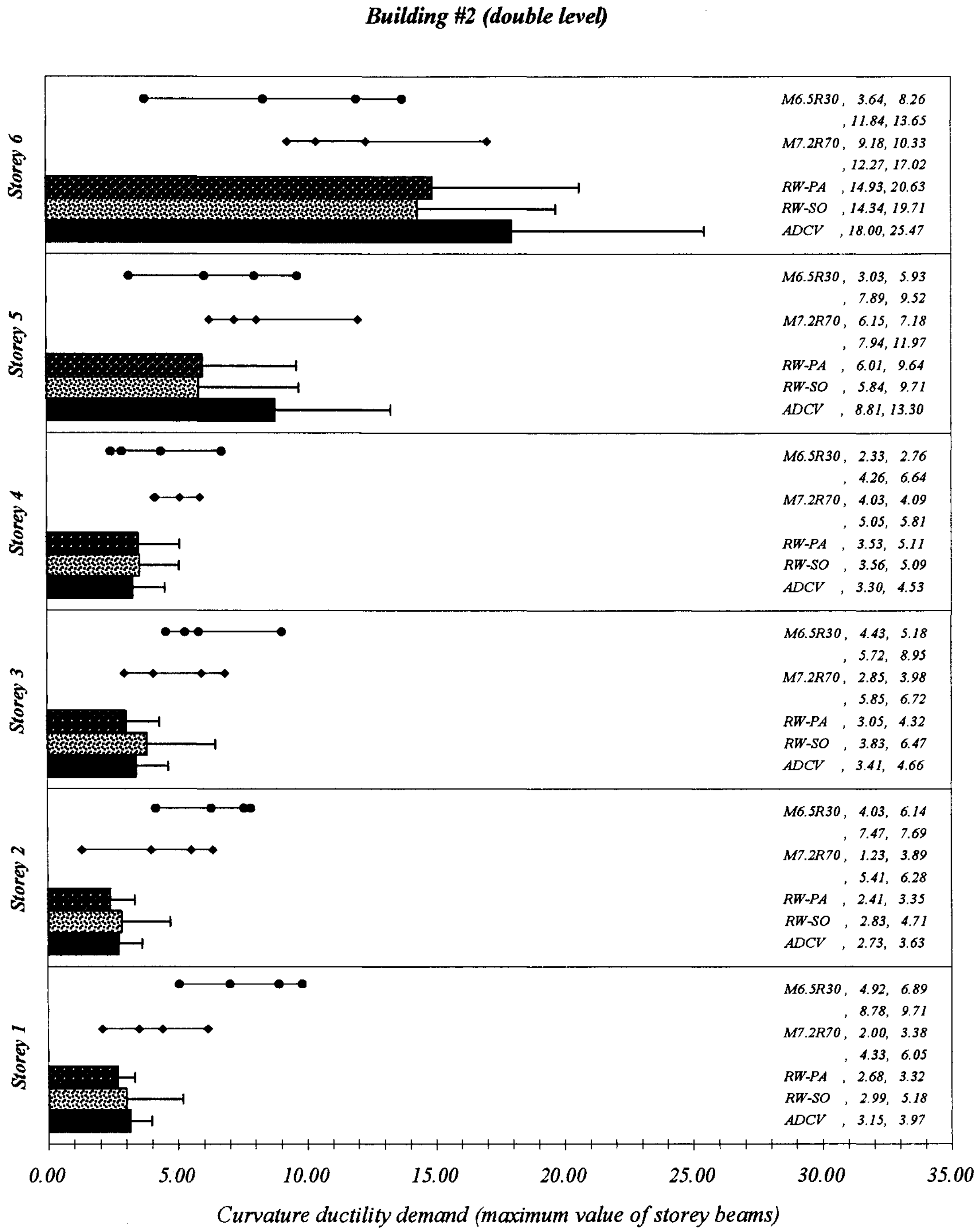

Fig. 6.13 Beam curvature ductility demands, Building #2, double level of excitation.

Maximum values of the mean and M+SD ductilities at each floor are presented for the ensembles of 15 accelerograms. The values for each of the four accelerograms of the simulated ensembles are shown.

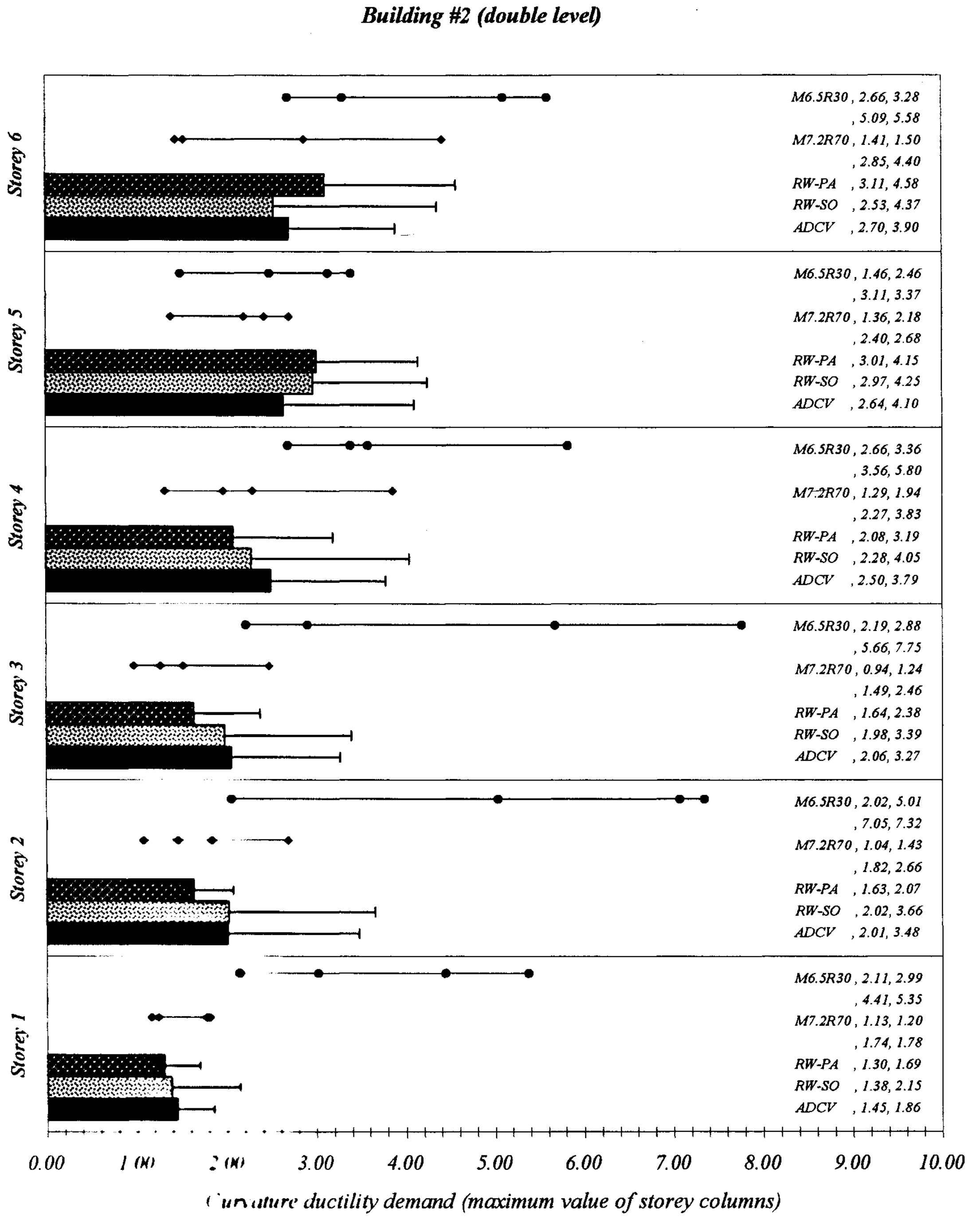

Fig. 6.14 Column curvature ductility demands, Building #2, double level of excitation.

Maximum values of the mean and M+SD ductilities at each floor are presented for the ensembles of 15 accelerograms. The values for each of the four accelerograms of the simulated ensembles are shown.

6.2.5 Results for Building #3, Normal Level of Excitation

The results for Building #3 for normal level of excitation are shown in Fig. 6.15 to Fig. 6.17. These figures show that the ensemble of Artificial Design spectrum Compatible accelerograms for Montreal (ADCM) and the ensemble of Real records for Eastern Canada scaled to Partial Area under the spectrum (RE-PA) give almost the same responses. On the other hand, the ensemble of Real records for Eastern Canada scaled to Spectral Ordinate (RE-SO) gives slightly larger responses than those of the ADCM and the RE-PA ensembles.

In any case, the values from all three ensembles are quite comparable. An explanation for this can be found by considering Fig. 5.8 (Montreal part) which shows that the mean spectra of the RE-SO and the RE-PA ensembles are very close to the design spectrum especially in the neighbourhood of the fundamental period of the building.

Figures 6.15 to 6.17 show that the results from the simulated stochastic accelerograms, M6.0R30 and M7.0R70 are quite close to those of the other three ensembles. This was expected for Building #3 because the simulated accelerograms for Montreal have spectra that are quite close to the design spectrum especially in the vicinity of the fundamental period of the building. Figure 5.3 shows that the stochastic simulated accelerograms for Montreal can be treated as compatible with the design spectrum, at least in the neighbourhood of the fundamental period of this particular building. This is the opposite of what was observed for the case of the simulated accelerograms for Vancouver (see Fig. 5.3).

The overall response of Building #2 when excited to normal excitation level is elastic. The reasons for this are the same as those discussed for Buildings #1 and #2 (see sections 6.2.1 and 6.2.3). It should only be mentioned here that the building was originally designed for a fundamental period of 0.71 and a lateral force of 6.86% of the overall weight of the building (see Table 3.5). On the other hand, the actual period of the building, as used in the dynamic analysis is 1.13 s. The seismic base shear corresponding to the period of 1.13 s is 3.66% of the weight of the building. This means the design seismic forces are 87% larger than the forces corresponding to the actual period of the building used in the analyses.

The maximum interstorey drifts at the mean and M+SD levels are 0.27% and 0.37% respectively. The maximum curvature ductilities in the beams are 0.44 at the mean level and 0.60 at the M+SD level. The ductilities in the columns are even smaller, and have the largest values of 0.19 at the mean level and 0.30 at the M+SD level.

In summary, the performance of Building #3 designed for Montreal, when subjected to earthquake motions compatible with the design spectrum (at least in the neighbourhood of the fundamental period) is purely elastic.

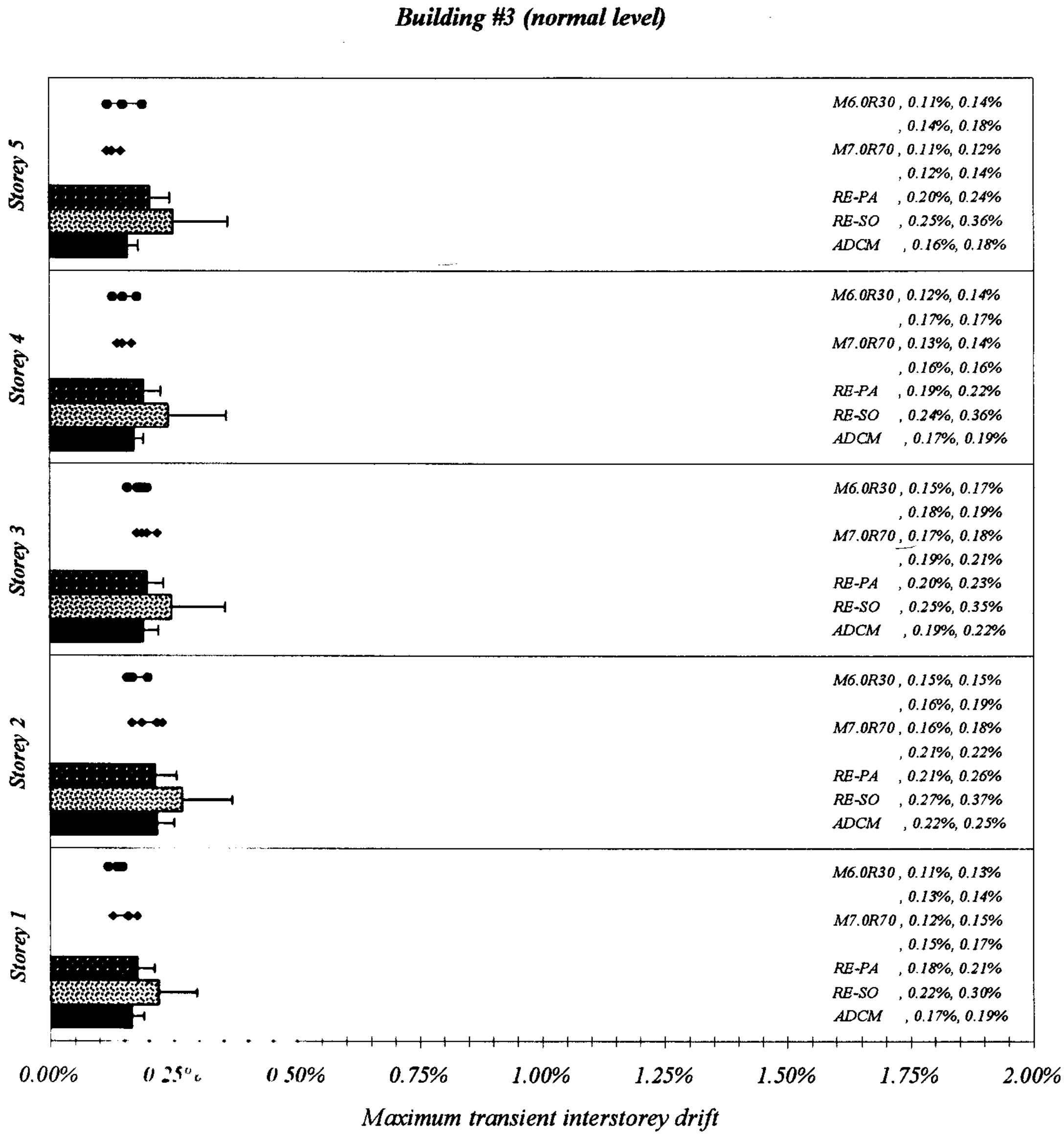

Fig. 6.15 Maximum transient interstorey drift, Building #3, normal level of excitation.

Mean and M+SD values are presented for the ensembles of 15 accelerograms. The values for each of the four accelerograms of the simulated ensembles are presented

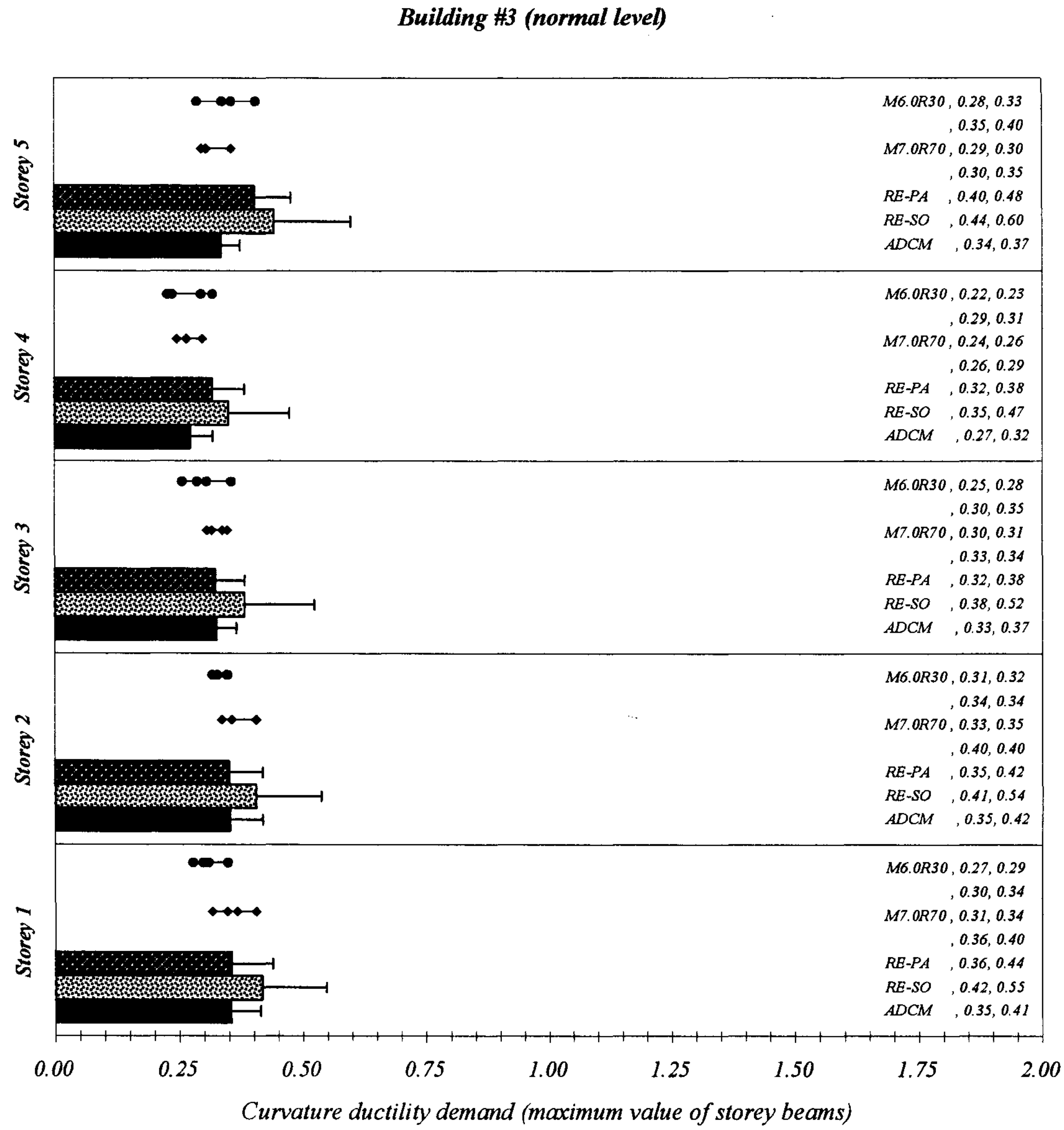

Fig. 6.16 Beam curvature ductility demands, Building #3, normal level of excitation.

Maximum values of the mean and M+SD ductilities at each floor are presented for the ensembles of 15 accelerograms. The values for each of the four accelerograms of the simulated ensembles are shown.

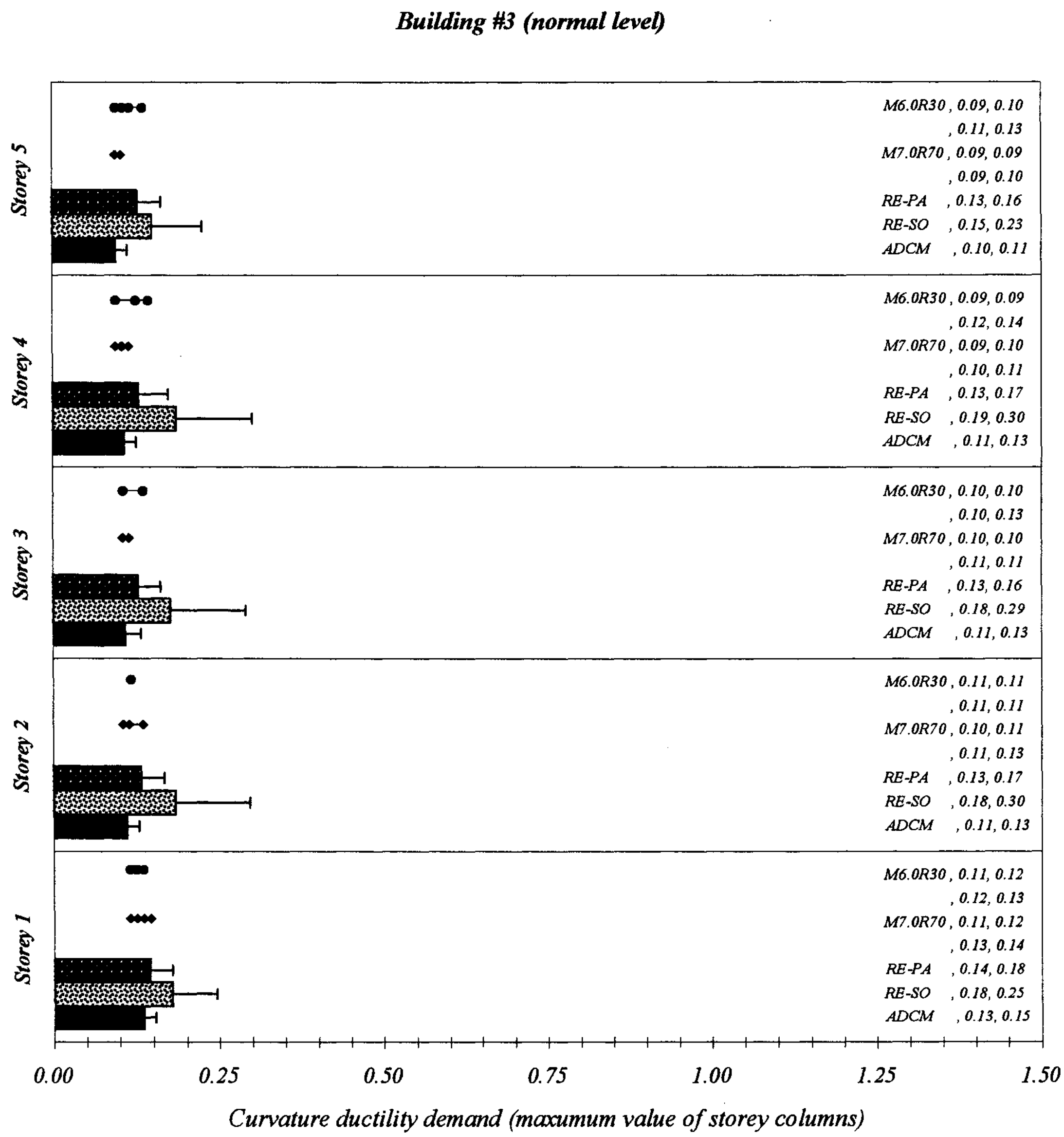

Fig. 6.17 Column curvature ductility demands, Building #3, normal level of excitation.

Maximum values of the mean and M+SD ductilities at each floor are presented for the ensembles of 15 accelerograms. The values for each of the four accelerograms of the simulated ensembles are shown.

6.2.6 Results for Building #3, Double Level of Excitation

The results for Building #3 for double level of excitation are shown in Fig. 6.18 to Fig. 6.20. The observations from these figures are the same as those for the normal level of excitation. Thus, the results from the dynamic analyses with Artificial Design spectrum Compatible accelerograms for Montreal (ADCM ensemble) and the Real records for Eastern Canada scaled to Partial Area (RE-PA ensemble) are quite close. The results from the dynamic analyses with the ensemble of Real records for Eastern Canada scaled to Spectral Ordinate (RE-SO ensemble) are somewhat larger than those from the analyses with the ADCM and the RE-PA ensembles. The results for the stochastic simulated accelerograms for Montreal (M6.0R30 and M7.0R70) are quite close to the mean responses of the ADCM, RE-PA and RE-SO ensembles.

Again, the response is purely elastic, i.e. both the column and beam ductilities are smaller than 1.0. Close examination of the responses shows that all the values (for drifts and ductilities) are almost double than those obtained from the analysis with the ensembles at normal level of excitation. This is expected, since the responses in both cases (normal and double excitation levels) are elastic.

The reasons for the elastic response even at the double excitation level are associated with the differences in the design base shear and that corresponding to the actual period of the building. As discussed in Section 6.2.5, the design base shear is 87% larger than that corresponding to the actual building period.

The maximum interstorey drift at the mean and the M+SD levels are 0.56% and 0.80% respectively. The maximum beam ductility at the mean level is 0.73 and at the M+SD level is 0.98. The largest column ductility is 0.45 at the mean level and 0.68 at the M+SD level. The maximum ductilities in the beams and columns are at the first storey.

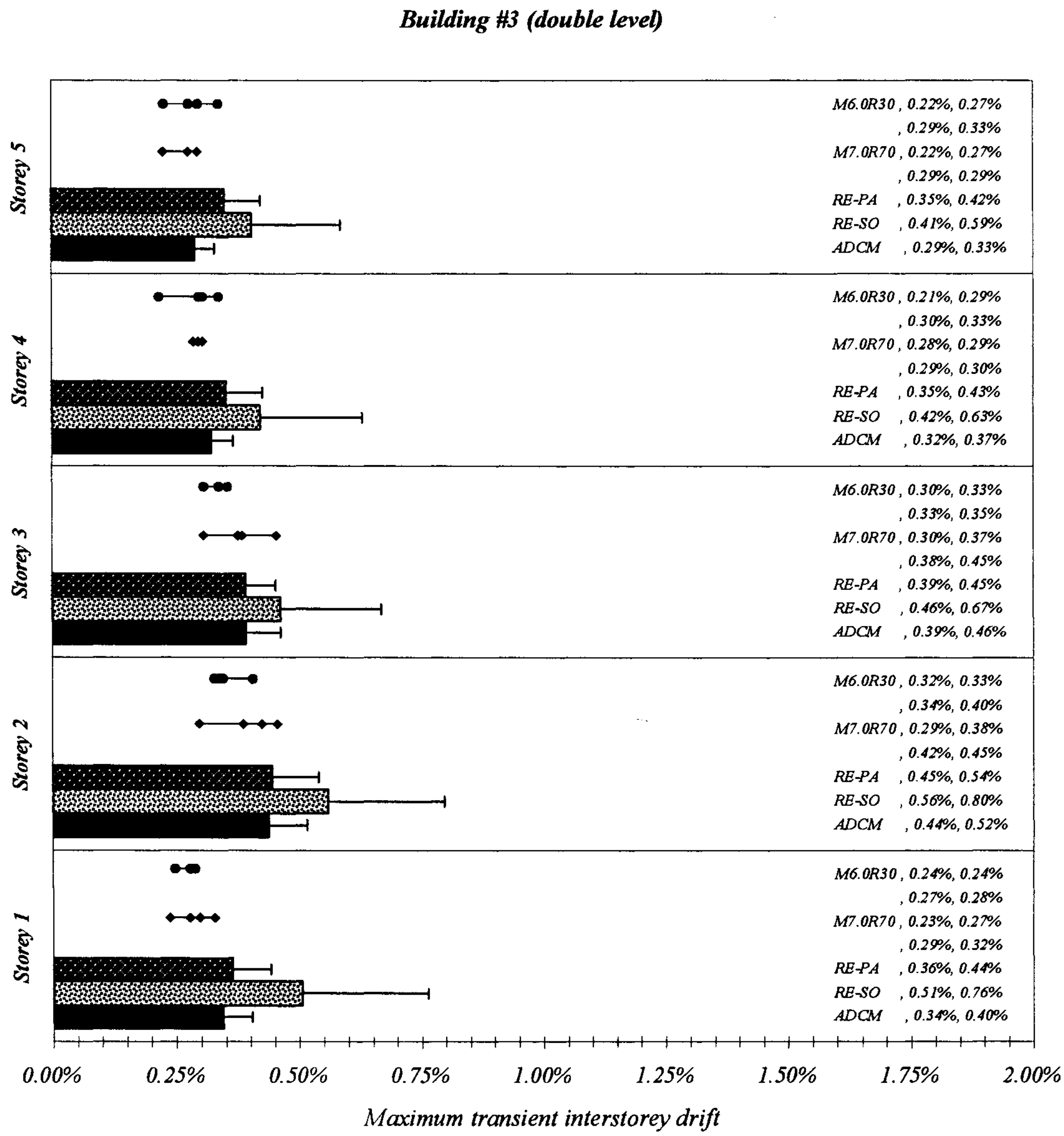

Fig. 6.18 Maximum transient interstorey drift, Building #3, double level of excitation.

Mean and M+SD values are presented for the ensembles of 15 accelerograms. The values for each of the four accelerograms of the simulated ensembles are presented.

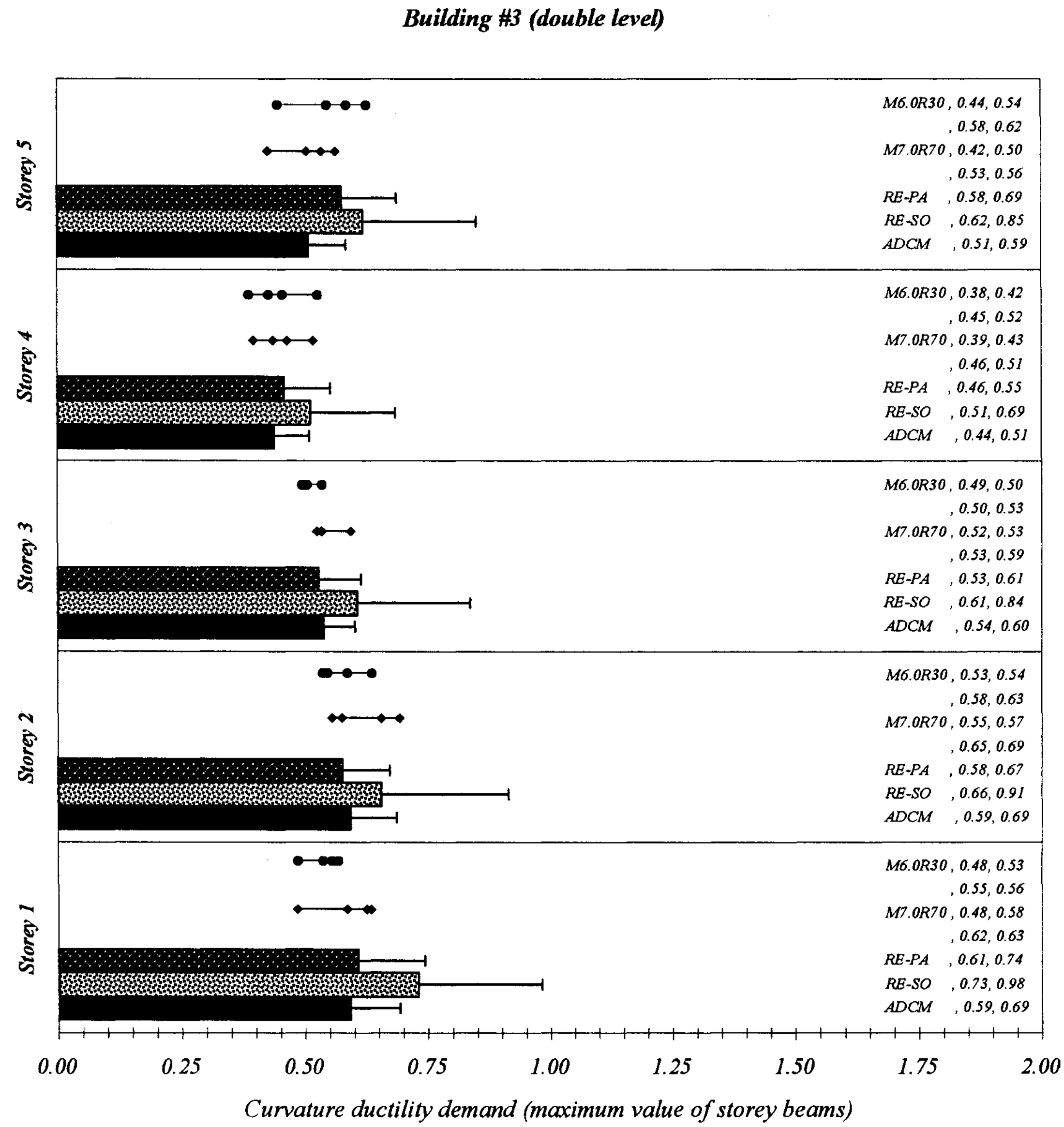

Fig. 6.19 Beam curvature ductility demands, Building #3, double level of excitation.

Maximum values of the mean and M+SD ductilities at each floor are presented for the ensembles of 15 accelerograms. The values for each of the four accelerograms of the simulated ensembles are shown.

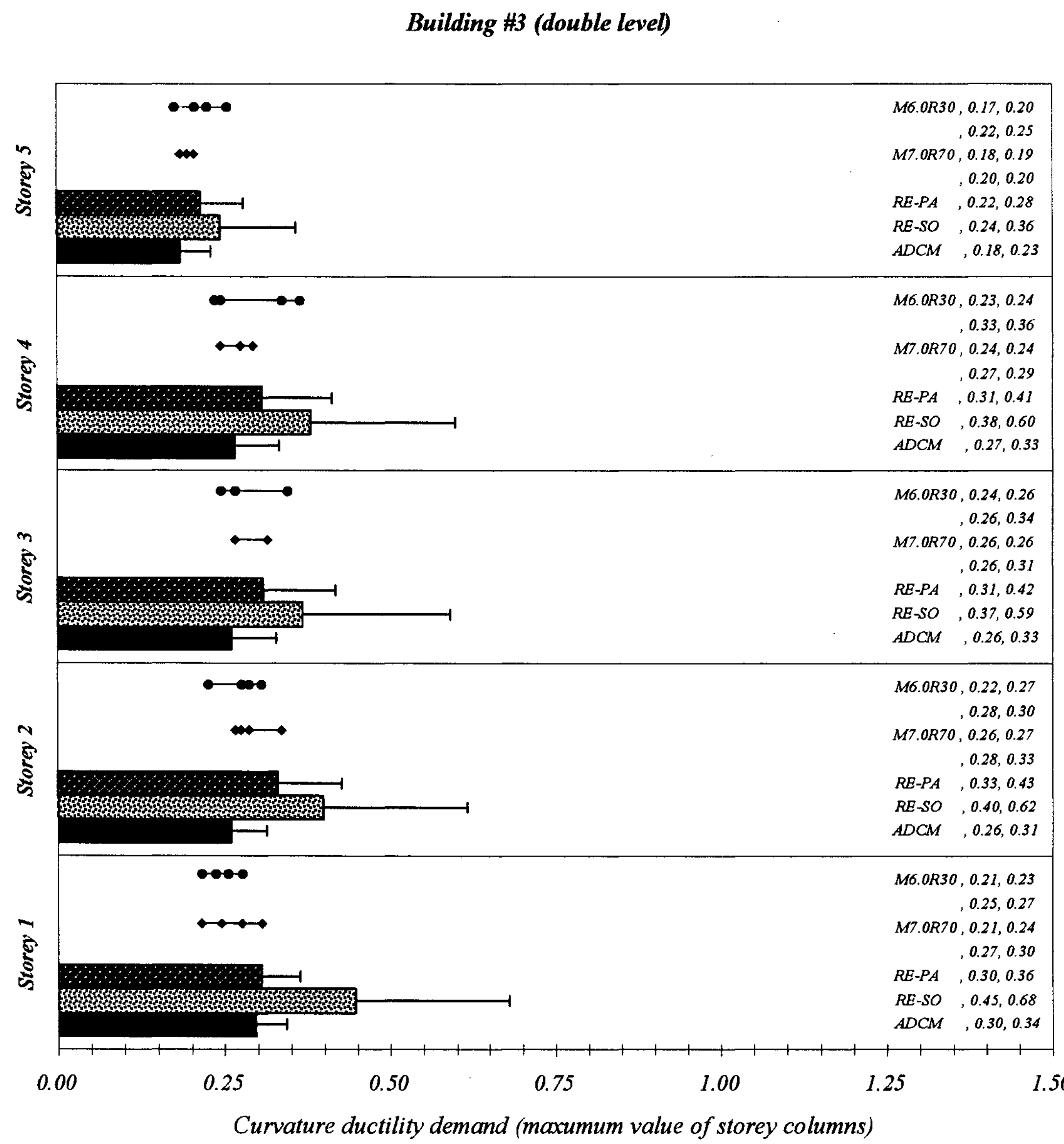

Fig. 6.20 Column curvature ductility demands, Building #3, double level of excitation.

Maximum values of the mean and M+SD ductilities at each floor are presented for the ensembles of 15 accelerograms. The values for each of the four accelerograms of the simulated ensembles are shown.

CHAPTER 7

DISCUSSION AND CONCLUSIONS

7.1 Summary

Modern seismic provisions of building codes specify seismic spectra for use in the design of buildings. Static seismic forces are directly related to these spectra which can be used for equivalent static analysis. The spectra can be also used in spectral analysis methods, when equivalent static forces corresponding to the predominant modes (i.e., the first several modes) can be directly expressed using the design spectra. However, for dynamic time-history analyses of building structures, acceleration time-histories of the ground motions compatible with the code spectra are required. The code explicitly requires that the design acceleration time-histories of the ground motions (referred to as design accelerograms) should be compatible with the design spectrum. While some codes specify certain criteria for the compatibility when real earthquake records are required by the code, in general the term "compatibility" is not defined by the codes and it is left to the designer to decide. Also, the codes do not specify what type of design accelerograms should be used, i.e. artificially generated to satisfy the design spectrum, or real accelerograms which can be scaled by some parameters in order to be close to the design spectrum. Currently, there are several methods and computer programs for generation of artificial accelerograms compatible with design (i.e. target) spectra, which are widely used in design of buildings. However, there are concerns in terms of the use of artificial accelerograms. Several research studies have indicated significant potential problems associated with the use of artificial accelerograms in the design of structures, which can distort the estimates of expected performance of the structures when subjected to design earthquake ground motions. In addition, with the use of artificial accelerograms, one of the most important feature of earthquake motions, i.e. the randomness of the motions, is lost.

The objective of this study is to evaluate the effects of various scaling techniques of real accelerograms on the response of medium height moment-resisting reinforced concrete frame buildings. Detailed time-history analyses were conducted on three reinforced concrete frame buildings. Two of these buildings were six-storey buildings located in Vancouver, one of which was a ductile moment-resisting frame, and the other one was a nominally ductile frame. The third building was a five-storey nominally ductile moment-resisting frame building located in Montreal. Two ensembles of real accelerograms recorded during strong earthquakes around the world were selected, one for Vancouver and the other for Montreal. Each ensemble contained 15 accelerograms. The frequency contents of the ensembles are representative for these two cities according to the 1995 edition of the seismic zoning maps of the National Building Code of Canada. Three scaling methods were used, i.e. (i) based on the spectral ordinate at the fundamental period of the building, (ii) based on the area under the spectral curve between the first and the second natural periods of vibration of the building (referred to as partial area), and (iii) based on the total area under the spectral curve throughout the whole period range (referred to as full area). Each scaling was conducted relative to the corresponding design spectrum (for Vancouver or Montreal) as given in the latest edition of the National Building Code of Canada (NBCC 2005). In addition to the real accelerograms, three ensembles of artificial accelerograms for Vancouver, and three ensembles for Montreal were used for the purpose of comparison. One of these ensembles contained 15 accelerograms that were generated to be compatible with the corresponding (for Vancouver or Montreal) design spectrum. Each of the other two ensembles of artificial accelerograms consisted of 4 stochastically simulated accelerograms. Two levels of excitations were used in the analyses, i.e. the design level according to NBCC 2005, and twice the design level.

The response parameters that were investigated in this evaluation study were the interstorey drifts, curvature ductility demands in the beams, and curvature ductility demands in the columns of the buildings. For each ensemble of excitation motions, statistical analyses were conducted to find the mean and the mean plus one standard deviation levels of the response parameters. The evaluation of the scaling methods of the real accelerograms was based on these two statistical levels.

7.2 Main Observations and Conclusions

The following are the main observations and conclusions from this study:

(1) The responses of the buildings resulting from excitation motions of real accelerograms scaled according to spectral ordinates and according to partial areas under the spectral curves were quite close for all three buildings, and for both levels of excitation.

(2) The scaling of the real accelerograms to the full areas under the spectral curves provided somewhat larger responses than those from the scaling to spectral ordinates and to the partial areas under the spectral curves.

(3) The generated artificial accelerograms compatible with the design spectra provided quite similar responses to those of the scaling to spectral ordinates and to the partial areas under the spectral curves.

(4) The simulated stochastic accelerograms were found to be not compatible with the design spectrum for Vancouver for all periods longer than 0.8 s; these accelerograms provided much larger responses than those of the other ensembles. In general, the overall shapes of the simulated stochastic accelerograms look like "rectangles" and are not representative of the shapes of real accelerograms.

7.3 Recommendations

The following are the main recommendations that can be drawn from this study:

(1) The excitation motions for use in time-history analysis of medium height reinforced concrete frame buildings should be represented by accelerograms obtained by any of the following three methods: (i) generated artificial accelerograms compatible with the design spectrum over the entire period range, (ii) real accelerograms scaled to partial area under the spectral curve within the predominant periods range, and (iii) real accelerograms scaled to the spectral ordinate at the fundamental structural period. Based on this study, the predominant periods range for medium height moment-resisting frame structures can be taken between the period of the second vibration mode and 1.2 times the period of the first vibration mode.

(2) The real accelerograms should have frequency content and strong motion duration that are representative of those of the expected seismic motions for the region where the structure is located. Because of the lack of recorded strong seismic motions in Canada, the real accelerograms can be selected from recorded motions during strong earthquakes in other regions in the world that have similar seismic and geotectonic characteristics to those of the building site. In the selection of the accelerograms, the frequency content can be assessed using the peak ground acceleration to peak ground velocity ratio (i.e., A/V ratios). In general, accelerograms with high frequency content ($A/V > 1$) are representative for eastern Canada, and accelerograms with intermediate frequency content ($A/V \approx 1$) are representative for western Canada.

7.4 Further Studies

The results from this study are representative for medium height reinforced concrete frame buildings. As mentioned above, the predominant periods range for medium height moment-resisting frame structures can be taken between the period of the second vibration mode and 1.2 times the period of the first vibration mode. Since the predominant periods range depends on the height of the building and its structural system, similar studies are needed for high rise frame buildings and other structural systems such as shear wall buildings, moment-resisting steel buildings, braced steel frames, and possible combinations of theses systems.

References

Adams, J., Weichert, D. H., and Halchulk, S. 1999, "Trial Seismic Hazard Maps of Canada-1999: 2% / 50 Year Values for Selected Canadian Cities", Geological Survey of Canada Open File 3274, National Earthquake Hazards Program, Geological Survey of Canada, Natural resources Canada, Ottawa, Ont.

Atkinson, G.M., Beresnev, I.A. 1998, "Compatible Ground Motion Time-histories for New National Seismic Hazard Maps", *Canadian Journal of Civil Engineering*, V 25, pp 305-318

Bayani-Keyvani, S. 2003, "Seismic Evaluation of Existing Reinforced Concrete Bridges in Ottawa Region", Master thesis, Department of civil engineering, University of Ottawa, Ottawa, Ont.

Chen, W.F., Scawthorn, C. 2003, *Earthquake Engineering Handbook*, CRC Press LLC, Boca Raton, Florida

Dincer, E. 2003, "'Seismic Drift Demands in Reinforced Concrete Structures", Master thesis, Department of civil engineering, University of Ottawa, Ottawa, Ont.

Eurocode 8 1998, European Committee for Standardization, "European Standard, Design of Structures for Earthquake Resistance, Part 2: Bridges", Brussels, Belgium

Filiatrault, A., Ladicani, K., and Massicotte, B. 1994, "Seismic Performance of Code-Designed Fiber Reinforced Concrete Joints", *ACI Structural Journal*, V. 91, pp 564-571

Filiatrault, A., Pineau. S., and Houde, J. 1995, "Seismic Behavior of Steel-Fiber Reinforced Concrete Interior Beam-Column Joints", *ACI Structural Journal*, V. 92, pp 543-552

GSC 2003, Geological Survey of Canada Open File 4459, "Fourth Generation Seismic Hazard Maps of Canada: Values for Over 650 Canadian Localities Intended for the 2005National Building Code of Canada"

Heidebrecht, A.C. 1995, "Insights and Challenges Associated with Determining Seismic Design Forces in A Loading Code", *Bulletin of the New Zealand National Society for Earthquake Engineering*, 28, pp 224-246

Heidebrecht, A.C. 1997, "Seismic Level of Protection for Building Structures", *Canadian Journal of Civil Engineering*, V 24, pp 20-23

Heidebrecht, A.C, Naumoski, N.1999, "Seismic Performance of Ductile Medium Height Reinforced Concrete Frame Buildings Designed in Accordance with the Provisions of the 1995 National Building Code of Canada", *Canadian Journal of Civil Engineering*, V 26, pp 606-617

Heidebrecht, A.C., Naumoski, N. 2002, "The Influence of Design Ductility on the Seismic Performance of Medium Height Reinforced Concrete Buildings". *American Concrete Institute, Special Publication*, SP-197, pp. 238-264

Heidebrecht, A.C. 2003, "Overview of Seismic Provisions of the Proposed 2005 Edition of the National Building Code of Canada", *Canadian Journal of Civil Engineering*, V 30, pp 241-254

ICBO 1991 & 1994, International Conference of Building Officials, *Uniform Building Code*, Whittier, California

Kunnath, S.K., and Reinhorn, A.M. 1992. "IDARC2D:Inelastic Damage Analysis of RC Building Structures", Technical Report NCEER-92-0022, National Center for Earthquake Engineering Research

Mander, J.B., Priestley, M.J.N., and Park, R. 1998. "Theoretical Stress-Strain Model for Confined Concrete", *Journal of structural Engineering*, ASCE, V. 114, No. 8, pp. 1804-1826

Mander, J.B., Priestley, M.J.N., and Park, R. 1998. "Observed Stress-Strain Behavior of Confined Concrete", *Journal of structural Engineering*, V. 114, No. 8, pp. 1827-1849

Martínez-Rueda, J.E. 1998, "Scaling Procedure for Natural Accelerograms Based on a System of Spectrum Intensity Scales", *Earthquake Spectra*, V. 14, No. 1, pp. 135-152

Naeim, F., and Lew, M. 1995, "On the Use of Design Spectrum Compatible Time-histories", *Earthquake Spectra*, V. 11, No. 1, pp. 111-127

Naumoski, N., Tso W.K., and Heidebrecht, A.C. 1988. "A Selection of Representative Strong Motion Earthquake Records Having Different A/V Ratios", EERG Report 88-01, Earthquake Engineering Research Group, Department of Civil Engineering, McMaster University, Hamilton, Ont.

Naumoski, N., Heidebrecht, A.C., and Rutenberg, A.V. 1993. "Representative Ensembles of Strong Motion Earthquake Records", EERG Report 93-1, Earthquake Engineering Research Group, Department of Civil Engineering, McMaster University, Hamilton Ont.

Naumoski, N. 1996, FIBER, "A Computer Program for Calculation of Moment – Curvature Relationships for Reinforced Members", (Not Published)

Naumoski, N., and Heidebrecht, A.C. 1997. "Seismic Level of Protection of Medium Height Reinforced Concrete Frame Structures, Design of Frames", EERG Report 97-1, Earthquake Engineering Research Group, Department of Civil Engineering, McMaster University, Hamilton, Ont.

Naumoski, N., and Heidebrecht, A.C. 1998a, "Seismic Level of Protection of Medium Height Reinforced Concrete Frame Structures, Member Properties for Seismic Analysis", EERG Report 98-1, Earthquake Engineering Research Group, Department of Civil Engineering, McMaster University, Hamilton, Ont.

Naumoski, N., and Heidebrecht, A.C. 1998b, "Seismic Level of Protection of Medium Height Reinforced Concrete Frame Structures, Modelling and Analysis", EERG Report 98-2, Earthquake Engineering Research Group, Department of Civil Engineering, McMaster University, Hamilton, Ont.

Naumoski, N. 2001, "Program SYNTH, Generation of Artificial Accelerograms Compatible with a Target Spectrum"

Naumoski, N. 2002a, "Artificial Accelerograms Compatible with the Uniform Hazard Spectrum for Vancouver", Research Report, Department of Civil Engineering, University of Ottawa, Ottawa, Ont.

Naumoski, N. 2002b, "Artificial Accelerograms Compatible with the Uniform Hazard Spectrum for Montreal", Research Report, Department of Civil Engineering, University of Ottawa, Ottawa, Ont.

NBCC 1995, "National Building Code of Canada", Institute for Research in Construction, National Research Council of Canada, Ottawa, Ont.

NBCC 2005 (draft version for review), "National Building Code of Canada", Institute for Research in Construction, National Research Council of Canada, Ottawa, Ont.

NZS 4203:1992, "Code of Practice for General Structural Design and Design Loadings for Buildings, Volume 1, Code of Practice", Standards New Zealand, Wellington, New Zealand

OSHPD 1991, California Office of Statewide Health Planning and Development, "An Acceptable Procedure for the Design and Review of California Hospital Buildings Using Base Isolation, Draft Revised April 26, 1991

Paulay, T., Priestley, M.J.N. 1992. *Seismic Design of Reinforced Concrete and Masonry Buildings*, John Wiley & Sons, Inc., New York, 744 p

Paulture, P. and Mitchell, D. 1987, "Evaluation of Seismic Performance of Concrete Frame Structures in Canada", Structural Engineering Series Report No. 87-4, Department of Civil Engineering an Applied Mechanics, McGill University, Montreal QC

Priestley, M.J.N., Seible, F., and Calvi, G.M. 1996, *Seismic Design and Retrofit of Bridges*, John Wiley & Sons, Inc., New York, 686 p

Shome, N., Cornell, C.A., Bazzurro, P., Carballo, J.E. 1998, "Earthquakes, Records, and Nonlinear Responses", *Earthquake Spectra*, V. 14, No. 3, pp. 469-500

Tremblay, R., Atkinson, G.M. 2001, "Comparative Study of the Inelastic Seismic Demand of Eastern and Western Canadian Sites", *Earthquake Spectra*, V. 17, No. 2, pp. 333-358